PN-ABK-259
75244

WORKING PAPER SERIES

# FISHERIES STOCK ASSESSMENT

## TITLE XII
## Collaborative Research Support Program

Fisheries Stock Assessment CRSP Management Office
International Programs, College of Agriculture
The University of Maryland, College Park, Maryland 20742

In cooperation with the United States Agency for International Development (Grant No. DAN-4146-G-SS-5071-00) the Fisheries Stock Assessment CRSP involves the following participating institutions:

The University of Maryland—Center for Environmental and Estuarine Studies
The University of Rhode Island—International Center for Marine Resource Development
The University of Washington—Center for Quantitative Sciences
The University of Costa Rica—Centro de Investigación en Ciencias del Mar y Limnología
The University of the Philippines—Marine Science Institute (Diliman)—College of Fisheries (Visayas)

In collaboration with The University of Delaware; The University of Maryland—College of Business and Management; The University of Miami; and The International Center for Living Aquatic Resources Management (ICLARM).

WORKING PAPER SERIES

Working Paper 86

# Particulate Theory of the Upper Ocean, Stochastic Geometry, Patch Structure, and Coupling With Physical Processes

by

B.J. Rothschild

June 1991

Fisheries Stock Assessment
Title XII
Collaborative Research Support Program

The Fisheries Stock Assessment CRSP (sponsored in part by USAID Grant No. DAN-4146-G-SS-5071-00) is intented to support collaborative research between the U.S. and developing countries' universities and research institutions on fisheries stock assessment and management strategies.

This Working Paper was produced by the University of Maryland-Center for Environmental and Estuarine Studies and the University of Costa Rica-Centro de Investigacion en Ciencias del Mar y Limnologia (CIMAR) in association with the University of Delaware and the University of Miami. Additional copies are available from the CRSP Management Office and from:

Chesapeake Biological Laboratory
Center for Environmental and Estuarine Studies
The University of Maryland
P.O. Box 38
Solomons, Maryland 20688

February 22, 1991

# PARTICULATE THEORY OF THE UPPER OCEAN, STOCHASTIC GEOMETRY, PATCH STRUCTURE, AND COUPLING WITH PHYSICAL PROCESSES

By

B. J. Rothschild

University of Maryland
Center for Environmental and Estuarine Studies
Chesapeake Biological Laboratory
Box 38
Solomons, Maryland 20688-0038

# Particulate Theory of the Upper Ocean, Stochastic Geometry Patch Structure, and Coupling with Physical Processes

By B. J. Rothschild

ABSTRACT . . . . . 1

INTRODUCTION . . . . . 3

STOCHASTIC GEOMETRY . . . . . 8
The Random Model . . . . . 9
Patch Models . . . . . 11
A transition from random structure to patch structure . . . . . 12
Random Closed Sets (RCS) . . . . . 14

APPLICATIONS TO PLANKTON BIOLOGY . . . . . 18
General Observations . . . . . 19
Molecule Donor and Acceptor Interactions . . . . 19
Grazing--The Structure of Phytoplankton Patchiness. . . . . 27
Micro-plankton and Grazer Search. . . . . 44

COUPLING WITH PHYSICAL PROCESSES . . . . . 50

COUPLING THEORY AND OBSERVATION . . . . . 55

DISCUSSION . . . . . 56

ACKNOWLEDGEMENT . . . . . 62

LITERATURE CITED . . . . . 68

# Particulate Theory of the Upper Ocean, Stochastic Geometry, Patch Structure, and Coupling with Physical Processes

by B. J. Rothschild

## ABSTRACT

Much of our understanding of upper-ocean community metabolism is derived from studies of primary production and calculations of mass-balance. These calculations alone cannot be used to understand the variability in the metabolic system. To understand metabolic variability, it is necessary to understand the phenomena that drive variability: population dynamics and trophodynamics. At the most fundamental level, population dynamics and trophodynamics involves the study of particle-particle interactions, where particles can range from photons and nutrient molecules, to microplankton (the very small heterotrophs and autotrophs), to the components of the more traditional food-chain. An important element governing the interactions among particles is the interparticle distance. The stochastic geometry or statistical distribution of interparticle distance is a measure of patch structure. First and second-order properties of the statistical distributions characterize interparticle distance. In particular, the second-order properties characterize the nature of patch structure; however, they are rarely taken into account. To

exemplify the theory of interparticle distance, the first and second-order properties of microplankton and phytoplankton patch structure are examined using both point process and random closed set (RCS) theory. Microplankton interparticle distances appear to be such that some are always proximal to one another, or to larger autotrophs, and hence capable of exchanging molecular nutrients, although the magnitude of the exchange depends upon factors external to geometric description. Phytoplankton patch structure is such that second-order statistics convey considerably more information on grazing conditions than the traditionally presented first-order numerical densities. The geometry of microplankton distribution may play an important role in enhancing chemosensory efficiency of grazer search. Stochastic geometry provides the link between the physical setting, trophodynamics, population dynamics, and hence community metabolism because it provides a natural linkage between distance-dependent physical phenomenon (such as homogeneous and isotropic turbulence) and trophodynamics.

## INTRODUCTION

Biological transformations associated with upper-ocean community metabolism (see Allee et al. 1949:495) have been the subject of considerable study. The transformation of nitrogen (from "new" and "regenerated" sources), carbon, and sunlight into primary production--the transformation of primary production into secondary production--catabolite and "cell leakage" exchanges between heterotrophs and autotrophs--and the net production of carbon dioxide and oxygen, are all well-known processes, as are other "biological-pump" non-metabolic components, sinking particulate matter and vertical migration (Jahnke, 1990; Longhurst and Harrison, 1989).

The biological transformations are the fundamental biological processes in the upper ocean. However, the theory representing the interactions among the transformations is not homogenous as it is represented by a complex of subcomponents, perspectives, or approaches. The complex can be exemplified by classifying the approaches: 1) ecosystem or community metabolism, 2) population dynamics, 3) trophodynamics, and 4) the physiology and behaviour of individual organisms (Figure 1). These approaches are not independent of one another--community metabolism integrates population dynamics, and population dynamics integrates trophodynamics, and trophodynamics integrates individual-organism physiology, and behaviour.

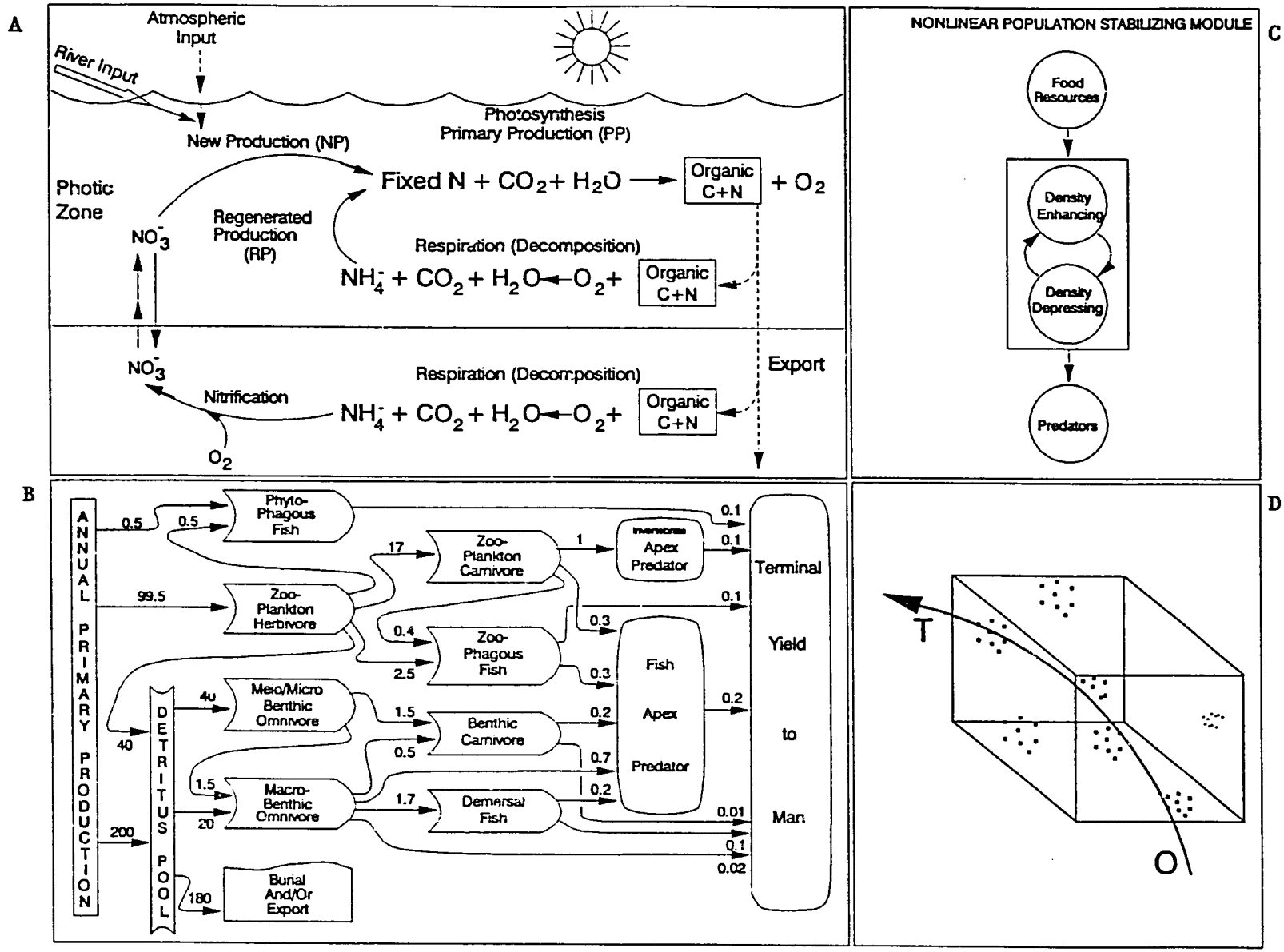


Figure 1. Hierarchical perspectives on upper ocean metabolism. Panel A is conceptual model of community metabolism (Jahnke, 1990). Panel B exemplifies a quantitative model of metabolism (Walsh, 1981). Panel C emphasizes the non-linear, density dependent components of population dynamics (Rothschild, in press). Note that the food resources and predator "arrows" can be viewed as "food signals". Panel D is example of a food signal sampled on the interval 0→T (Rothschild, 1988).

The integrative relationship can be characterized as a nested hierarchy. The hierarchy represents a set of coherent processes and different epistemological approaches. One approach is aggregative, relating to community-metabolism, mass-balance, and input-output considerations. The other approach is disaggregative, or particulate, relating to the allocation of biomass or bioactive material to individual organisms and non-living bioactive particles. The hierarchical arrangement implies that the quality of understanding of community metabolism depends upon the quality of understanding of the subsidiary hierarchical levels.

Accordingly, to understand variability in community metabolism, it is necessary to understand the way variability (and symmetrically, stability) is propagated or damped by population dynamics or trophodynamics. The reverse is of course true, to understand population dynamics and trophodynamics it is necessary to understand the constraints of community metabolism in the allocation of biomass to living and non-living particles.

From a particulate point of view, the foundations for understanding variability in upper-ocean community metabolism are represented by a scant literature. The foundation is built upon the population-dynamics process (e.g. Rothschild 1986: Chapter 8) The process operates at the particulate level and paces the stochastic trajectory of metabolic input-output relationships. The process is driven by trophic transactions. The transactions are measured in terms of the temporal distribution of ingestion rates which depend upon predator-prey encounter rates (Rothschild and

Osborn 1988; Gerritsen and Strickler 1977).

The predator-prey encounter rates depend upon the relative numerical density, the relative velocity, and kinetic-structure-modified relative velocity of predator and prey. However, even the understanding of the relative density and relative velocity of predator and prey has generally been limited to first-order properties of predator-prey relative density, even though the "patch structure" second-order properties generally contain substantial information on encounter rates.

Considering only first-order properties implies that living and bioactive particles are distributed randomly--that is, a patch structure does not exist; interparticle distance is consonant with the Poisson process. Assuming that particle distribution is Poisson or random, when it is not, distorts our understanding of 1) the magnitude of predator-prey interactions; 2) trophodynamics biology; 3) the linkage between trophodynamics and population dynamics; and 4) the coupling between trophodynamics and physical processes.

The statistical distribution of particles and their first and second-order properties involves the study of particle geometry. Because geometry is well defined and unambiguous it is easily linked with computer and field experiments. It is also easily linked with empirical endeavors and an important component in the design and sampling theoretical deployment of sensors because sensors (e.g. plankton nets, acoustics, and optical devices) all measure statistical functions of plankton geometry. Because geometry specifies the position of each living or bioactive non-

living particle, it also specifies interparticle distance, a fundamental property of trophodynamic interrelationships, and a fundamental metric that links the elements of the subcomponents in the theoretical hierarchy.

This paper considers the rudiments of a particulate theory of the upper ocean in the context of interparticle distance. The notions of interparticle distance are contained in the theory of stochastic geometry. The theory enables taking account of, the transition of particle distribution from random to patchy, and biological "feeding scales", rather than anthropocentric sampling scales.

The first part of the paper brings together the essential elements of stochastic geometry. The second part presents a geometric viewpoint regarding 1) heterotroph-autotroph, 2) grazer-autotroph, and 3) small microplankton-grazer interactions. The third part of the paper shows how stochastic geometry is a requisite for analysis of the coupling between biological and physical processes. The fourth part discusses the way that stochastic geometry facilitates a coupling with dynamic theory and empirical activities.

The geometrical analysis of plankton distribution reflects the need to revise models that do not take account of <u>quantitative</u> patchiness and sets the stage for linking basin-scale changes in the wind field with microscale feeding conditions and associated population dynamics. Obviously an understanding of interparticle distance is an essential ingredient to understanding how

variability in community metabolism interrelates with the "biological pump", the analysis of primary and secondary production, the causes of very large year classes of fish, the fate-and-effect of anthropogenic substances, and the design of sampling technology.

## STOCHASTIC GEOMETRY

An approach to the study of the particulate foundations of community-metabolism variability involves considering the biota of the upper ocean as a collection of stochastic points. The points are particles with dynamic properties representing living or otherwise bioactive particles. Each point is a locus of biodynamic transformation--phytoplankton cells transform photons and nutrient molecules into biomass and copepods remove phytoplankton cells from the environment, and convert the cells into anabolites, catabolites, and pellets, etc.

The intensity of the transformational properties of particles are fueled by particle-particle interactions. The propensities for particles to interact is a function of interparticle distance. Interparticle distance is a function of particle distribution. Particle distribution and the metabolic function partition N(n), can be written,

$$\Psi = \{X_i ; \delta_j (X_i)\},$$
$$N(n) = \sum_{j=1}^{m} n_j = N \qquad (1)$$

where $X_i$ is the three-dimensional stochastic position of the $i=1,\ldots,N$ particles, $\delta_j(X_i)$ is the j-the metabolic function $j=1,\ldots,M$ of the i-the particle, and $n_j$ is the number of particles having the j-the metabolic function.

There are many possible classifications of $\delta_j$. These classifications can be taxa, size, location, etc., specific. One simplified classification of metabolic function might be j=1, micro-autotroph; j=2, micro-heterotroph; j=3, large autotroph; j=4, large grazer; j=5, predator.

The geometry implied by Eq(1) can be studied via both point-process and random closed set (RCS) theory. To our knowledge RCS theory has never been applied to plankton distributions. Our discussion of RCS is based on Stoyan, Kendall, and Mecke, 1987. First we draw on the theory of random distributions. We then describe the notion of patch structure using the patch structure of a mixed Poisson-point process and RCS theory.

**The Random Model**

The random or Poisson probability distribution implies that the probability distribution function of the distance to the nearest neighbor (see e.g. Pielou 1977) is,

$$D_R(r) = 1 - \exp\left(-\frac{4}{3}\lambda\pi r^3\right), \qquad (2)$$

where $\lambda$ is the mean density of particles in three-dimensional space

and r is the nearest-neighbor distance between particles. The derivative of Eq(2) yields the probability density function,

$$D_R'(r) = 4\lambda\pi r^2 \exp\left(-\frac{4}{3}\lambda\pi r^3\right). \tag{3}$$

which enables calculation of the mean nearest neighbor distance, NND,

$$\bar{r} = 4\lambda\pi\int_0^\infty r^3 \exp\left(-\frac{4}{3}\lambda\pi r^3\right) dr \tag{4}$$

Integration of Eq(4) (see Appendix I) yields the NND,

$$\bar{r} = .55\lambda^{-1/3} \tag{5}$$

It is important to recognize that $\bar{r}$, is an average value. This means that when $\bar{r}$ is used to appraise interactions among particles, roughly half of the interactions will be based upon distances that are less than $\bar{r}$, and half the interactions will be based on distances greater than $\bar{r}$.

However, distances other than the mean distance are important for some purposes. As an example, consider the <u>minimum</u> mean distance to the nearest neighbor, MNND. The theory of order statistics is used to compute the MNND. N independent NND's are measured and ranked from smallest to largest to obtain $R_1, R_2, \ldots R_N$. Instead of $\bar{r}$, the mean distance to the nearest neighbor, we are now interested in $\bar{r}^*$, the mean <u>minimum</u> distance to the nearest neighbor. The mean of the minimum of all $R_i$ observations, $R_1$ (as distinct from the distribution of the random variable R) is obtained from the general formula for the probability density

function for the minimum value of order statistics,

$$D_R(r_1) = n[1-D_R(r)]^{n-1} D_R'(r), \tag{6}$$

using Eq(2) and Eq(3) in Eq(6) we have,

$$D_R(r_1) = 4n\lambda\pi r^2 \exp\left(-\frac{4}{3}n\lambda\pi r^3\right). \tag{7}$$

calculating the mean from Eq(7), we have,

$$\bar{r}^* = n4\lambda\pi \int_0^\infty r^3 \exp\left(-\frac{4}{3}n\lambda\pi r^3\right) dr \tag{8}$$

The integral of Eq(8) is,

$$\bar{r}^* = .55\, n^{-1/3} \lambda^{-1/3} \tag{9}$$

In other words, as n increases, the mean MNND decreases. We are led to the conclusion that if we are interested in average distances then $\bar{r}$ is the appropriate statistic. On the other hand, if we are interested in how close distances might be, given n, then $\bar{r}^*$ is appropriate. Inasmuch as there is always a very large number of particles, and a large number of independent distances, some interparticle distances can be made to be arbitrarily small at any instant of time.

**Patch Models**

There is only one Poisson-process or random model (with several versions). In contrast, there are several classes of patch-structure models (see e.g. Fasham 1978a, 1978b). However, to determine the most appropriate class is difficult using only empirical data. The alternative, selecting a class of patch-

structure models from first principles is equally problematic, since the first principles are not as yet well understood. Nevertheless, much of the qualitative flavor of the patch-structure problem can be gleaned from simple examples. For this reason, we present two different types of patch models, a point-process mixed-Poisson model and a RCS model. These examples enable qualitative appraisal of the nature of patchiness, pending a more detailed study of mechanisms.

<u>A transition from random structure to patch structure</u>. As a special case, the <u>mixed</u> Poisson distribution is a patch structure model containing the random, non-patch structure, Poisson distribution. The mixed Poisson distribution is a mixture of a low-density Poisson parameter $\lambda_1$ and a high density Poisson parameter (i.e. $\lambda_1<\lambda_2$). Thus $\lambda_2$ can be thought of as an intrapatch density while $\lambda_1$ can be thought of as an interpatch density. It should be obvious that the mixed Poisson distribution does not result in patches per se but rather point-wise, independent, high and low densities. The mixing parameter is $\nu$ so $\lambda_1$ is specified to occur with probability $(1-\upsilon)$ and $\lambda_2$ with probability $\upsilon$ (for a detailed analysis of this process in connection with the biological functional response, see Rothschild, submitted). The random special case is obtained by letting $\lambda_1=\lambda_2$. Also, as $\upsilon$ approaches zero or 1, the mixed Poisson distribution approaches the random or Poisson distribution.

The intensity of the process is,

$$\bar{\lambda} = (1-\nu)\lambda_1 + \nu\lambda_2, \tag{10}$$

The NND distribution function is,

$$D(r) = \bar{\lambda}^{-1}[\lambda_1(1-\nu)(1-e^{-\lambda_1\omega r^3}) + \lambda_2\nu(1-e^{-\lambda_2\omega r^3})] \tag{11}$$

where $\omega = \frac{4}{3}\pi$. The probability density function is derived from Eq(11),

$$\begin{aligned} D'(r) &= 3\alpha\lambda_1\omega r^2 e^{-\lambda_1\omega r^3} + 3\beta\lambda_2\omega r^2 e^{-\lambda_2\omega r^3} \\ \alpha &= \bar{\lambda}^{-1}\lambda_1(1-\nu),\ \beta = \bar{\lambda}^{-1}\lambda_2\nu \end{aligned} \tag{12}$$

Accordingly the mean NND is,

$$\begin{aligned} \bar{r} &= 3\omega\int_0^\infty \left[\alpha\lambda_1 r^3 e^{-\lambda_1\omega r^3} + \beta\lambda_2 r^3 e^{-\lambda_2\omega r^3}\right]dr \\ &= .55\bar{\lambda}^{-1}\left[(1-\nu)\lambda_1^{2/3} + \nu\lambda_2^{2/3}\right] \end{aligned} \tag{13}$$

The reduced second order moment function (RSOMF) is,

$$K(r) = \left[\frac{\lambda_1^2(1-\nu) + \lambda_2^2\nu}{\lambda_1(1-\nu) + \lambda_2\nu}\right]\left[\frac{4}{3}\pi r^3\right] \tag{14}$$

The product of the mean density $\bar{\lambda}$ and the reduced second order moment function gives the expected number of particles, a distance less than r.

If distributions are random then <u>all</u> of the information on the distribution is contained in the mean. If, however, distributions are patchy, then the second-order properties of the distribution need to be considered. To emphasize this point in a patchy distribution, in contrast to a random distribution, knowing the over-all mean, $\bar{\lambda}$, does <u>not</u> imply unique value for $\bar{r}$, the NND.

**<u>Random Closed Sets (RCS)</u>**. The theory of random closed sets can be used to take a different approach to spatial-patch distribution.

A RCS is defined as,

$$\Xi = (\Xi_1 + x_1) \cup (\Xi_2 + x_2) \cup \ldots \cup (\Xi_N + x_N) \tag{15}$$

where $x_i$ is the position in 3-dimensional Euclidean space of the i-the particle and $\Xi_i$ is a random closed set associated with $x_i$. The $x_i$'s are called the "germs" of the process while a typical $\Xi_i$, $\Xi_o$ is called a "primary grain" (note that $\Xi_o$ is not one of the $\Xi_i$'s). If $\phi = \{x_1, x_2 \ldots\}$ is a statistically stationary Poisson process and if the primary grains can be considered as closed sets, then $\Xi$ is called a Boolean model. The first and second order properties of the Boolean model are well known.

For our application we consider the primary grain to be a sphere with radius r. The radius of the sphere is taken as a random variable.

We might think of each random sphere as a collection of particles enclosed by the sphere perimeter. The particles inside the spheres have equal density, or some minimum density, or densities which are functions of the sphere radius. The spheres can be thought of as "spheres of influence". If a particle from a particular sphere of influence is inside the sphere of influence of another particle, then there is a potential for interaction between the two germs or particles.

Given that the germs are randomly distributed with intensity $\lambda$ and that the primary grain is a sphere with normally distributed radius $N(\mu, \sigma^2)$, and hence third moment, $3\mu\sigma^2 + \mu^3$., we can examine a) the volume fraction b) the parameter of the chord length distribution c) the contact distribution and d) the covariance function. We observe here that the normal distribution is used for heuristic purposes, technically having no lower bound, its replacement by a gamma distribution (for example) would be more rigorous. In addition, very large variances mimicking larger-scale and more complex patch structure could be more comfortably accommodated with the gamma distribution.

The volume fraction or the percentage of the volume occupied by $\Xi$ with the parameter set $\Xi(\lambda, \mu, \sigma^2)$. is,

$$p = 1 - \exp\left(-\frac{4}{3}\lambda\pi\left(3\mu\sigma^2 + \mu^3\right)\right) \tag{16}$$

where $\lambda$ is the intensity of the "germs" and $3\mu\sigma^2 + \mu^3$ is the third moment associated with the normally distributed radius of the primary grain. Inspection of Eq(16) reveals that an increase in

any of the parameters increases the volume fraction.

The volume fraction statistic p requires careful interpretation. When p is small there is only a small chance of overlap in the primary grains. However, as p becomes large the chance of overlap increases. So the Boolean model really represents two patch modalities: i, for small p the patchiness results from confining particles to spheres; ii, for large p patchiness is complex in the sense that patchiness results from confining particles to spheres and from the intersection of spheres where the densities of particles are at least doubled. It is important to recognize that the probability of a sphere being isolated (i.e. not overlapped by another sphere) is not symmetrical with the volume fraction.

A "mean free" path among the spheres can be deduced. The chord lengths between spheres is exponentially distributed with parameter

$$L = \lambda \pi \mu \tag{17}$$

This is the parameter of the familiar waiting-time distribution and enables modeling interactions among the particles as a stochastic process. In particular Eq(17) has important applications in reduced-dimensionality problems. One example involves a large phytoplankton cell sinking through a three-dimensional volume. Another involves the penetration of a light beam through the volume (having applicability in situ or in remote sensing).

The spherical contact distribution is given as,

$$H(r) = 1-\exp(-\lambda\pi r(4(\sigma^2+\mu^2)+4\mu r+\frac{4}{3}r^2)) \tag{18}$$

This is the distance to the nearest sphere from a randomly chosen point outside a sphere. Accordingly H(r) gives a measure of one-dimensional "void space" from a randomly selected three-dimensional vantage point, not in a sphere of influence.

Finally, the covariance function specifies the distribution of distances between points (as distinct from germs) within <u>and</u> among spheres.

$$C(r) = 2p-1+(1-p)^2\exp\left[\frac{4}{3}\lambda\pi\int_{r/2}^{\infty}x^3\left(1-\frac{3r}{4x}+\frac{r^3}{16x^3}\right)dF_r(x)\right], \tag{19}$$

where

$$dF_r(x) = \frac{1}{\sigma\sqrt{2\pi}}\exp-[(x-\mu)^2/2\sigma^2], \tag{20}$$

because r is $N(\mu,\sigma^2)$. The covariance function characterizes the spacing among germs and primary grains. Note that the maximum value of the covariance function is p and the minimum value is asymptotically $p^2$. In a sense the covariance measures the rapidity with respect to r that the covariance declines, which is a measure of the "redness" of the variability at feeding scales.

Note that the covariance function can be used to define an integral feeding scale,

$$F = \int_0^{\infty}C(r)\,dr \tag{21}$$

the scale F, might be perceived by a predator feeding among prey

with specified germ and typical grain distributions. F is a natural coupling with feeding biology in the context of the theory of homogenous and isotropic turbulence.

The theory of random closed sets easily lends itself to considering certain aspects of the intersections among RCS. For example, consider the joint volume fractions and covariance functions,

$$P = \prod_{i=1}^{N} p_i$$
$$C(r) = \prod_{i=1}^{N} C_i(r) \tag{22}$$

When N=2; i=1 could refer to a predator; and i=2, to a prey. Larger N could represent various scales of patchiness. Formulations such as Eq(22) permit considerable flexibility.

## APPLICATIONS TO PLANKTON BIOLOGY

The purpose of this section is to exemplify the theory of stochastic geometry in the study of plankton. We 1) make some general observations, 2) consider interactions among micro-plankton, 3) grazing and 4) grazer/micro-plankton interactions.

At the outset it should be clear that at present it is difficult to apply "real numbers" to the theory. This is because 1) the knowledge of anabolic-catabolic kinetics of microplankton is limited, 2) most reports or particle-particle interaction are based on units such as chlorophyll quantity or concentration rather than particles, and 3) those numerical densities that are given are difficult to interpret because they are reported only as first-order statistics.

**General Observations**

It is remarkable that among the major groups of phytoplankton there is little overlap between the distributions of interparticle distances (at least for the major functional groups). In fact it might be said that in the upper ocean various functional groups appear to have a canonical distribution of densities and size. That is, the larger zooplankton (order of $10^{-2}$ $cm^{-3}$ in number, and 1000 $\mu m$ in diameter) are about 10 times larger than the larger phytoplankton (order of 100 $cm^{-3}$ in number and 10 $\mu m$ in diameter) which are 10 times larger than the microplankton (order of $10^{6}$ $cm^{-3}$ in number and 1 $\mu m$ in diameter). Accordingly, there is a large separation between the NND of each group. These separations are also carried into the MNND. It is also remarkable that the microplankton are so close to one another, and the zooplankton are so large, that zooplankton must be in continual contact with microplankton (Figure 2).

**Molecule Donor and Acceptor Interactions**

Interactions among molecular donors and acceptors (the small and large autotrophs and the small heterotrophs) are complex and hardly understood. Part of the complexity is that each of these particles is a molecular-nutrient acceptor and a molecular-nutrient donor. Molecular-nutrient donors range from microbial to the largest organisms. Molecular-nutrient acceptors are autotrophs ranging in size from 1 $\mu m$ to perhaps 50 $\mu m$ in diameter and heterotrophs which are perhaps no larger than 5 $\mu m$.

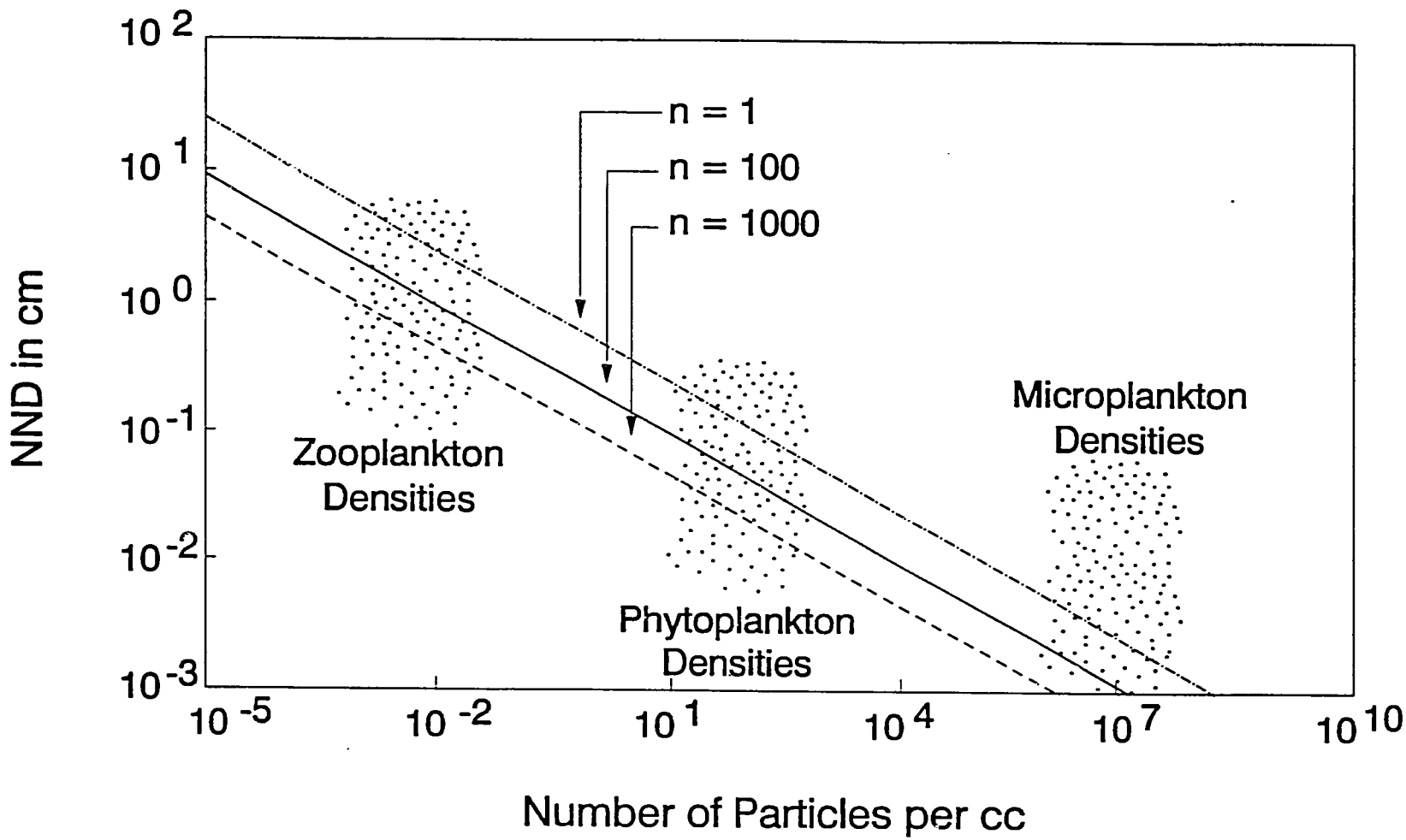


Figure 2. Nearest neighbor distance (NND) as found in particle density. The line corresponding to n=1 is the conventional NND. The lines corresponding to n=100 and n=1000 are MNND's for n=100 and n=1000 respectively. Typical ranges of numerical densities (which generally do not overlap) are shown for zooplankton, phytoplankton, and microplankton.

There is evidently considerable uncertainty with regard to donation of nutrient molecules. These uncertainties involve specific chemical properties of the molecules, their temporal production, and the extent to which they result from catabolism, cell leakage, or feeding debris. In addition, the physical-chemistry governing the fate of the molecules is hardly understood involving interactions between molecular diffusion and turbulent flow or remnants of turbulent flow.

A key problem in evaluating interactions between donors and acceptors is the typical modality by which molecules are transferred by donors to acceptors. There are two distinct points of view (see Jackson, 1987, for review). One is that donors and acceptors are sufficiently close that exchanges occur at nutrient concentrations greater than at diffused background levels. The other is that particles are so far apart and diffusion is so rapid that nutrient exchanges occur only at diffuse background levels.

The distance between donors and acceptors is thus a key issue in considering the modality of interaction among micro-organisms.

The problem might be studied by focusing on the spatial distribution of micro-plankton as might be perceived by a random point occupied by an autotroph. We assume that there are $1.5 \times 10^6$ micro-plankton $cm^{-3}$; that each micro-plankton has a radius of 1 $\mu m$; and that the autotroph has a radius of 10 $\mu m$. Accordingly, the NND among random points with density $1.5 \times 10^6$ is 48 $\mu m$.

This means that the <u>average</u> distance between cell walls is 37 $\mu m$. The probability distribution function corresponding to these

specifications is shown in Figure 3. Roughly one-half the microplankton cells are within 37 $\mu$m of the autotroph cell wall. Taking expectations, p=.06 percent of the nearest neighbor distances are as close as 10 $\mu$m distant from the autotroph. This is 90,000 nearest neighbor distances. Examination of the RSOMF shows that on the average 6 cells are in a shell having inside diameter of about 50 $\mu$m and an outside diameter of about 100 $\mu$m (Figure 4). This is of interest because while on one hand there are <u>on the average</u> six cells within 100 $\mu$m of a typical cell, there are on average no cells within 50 $\mu$m. It is reasonable to expect that of these, half will be closer than the NND to each other and hence could increase the local density of catabolites. On consideration of the probability distribution of NND and the MNND in the random case, it is likely that at any fixed instant some autotrophs and heterotrophs are sufficiently close to exchange or transmit metabolites at concentrations in excess of background levels, a line of reasoning certified by the MNND type of calculation, yet potentially flawed by a lack of understanding of catabolite kinetics.

RCS theory can be specifically applied to the sphere of influence or microzone (Mitchell et al) around each particle. Mitchell et al give the radius of a microzone,

$$r = \frac{Q}{4\pi DC} \tag{23}$$

where Q is the total nutrient flux per cell, D is the molecular diffusivity and C is threshold concentration (they set C=.10) above

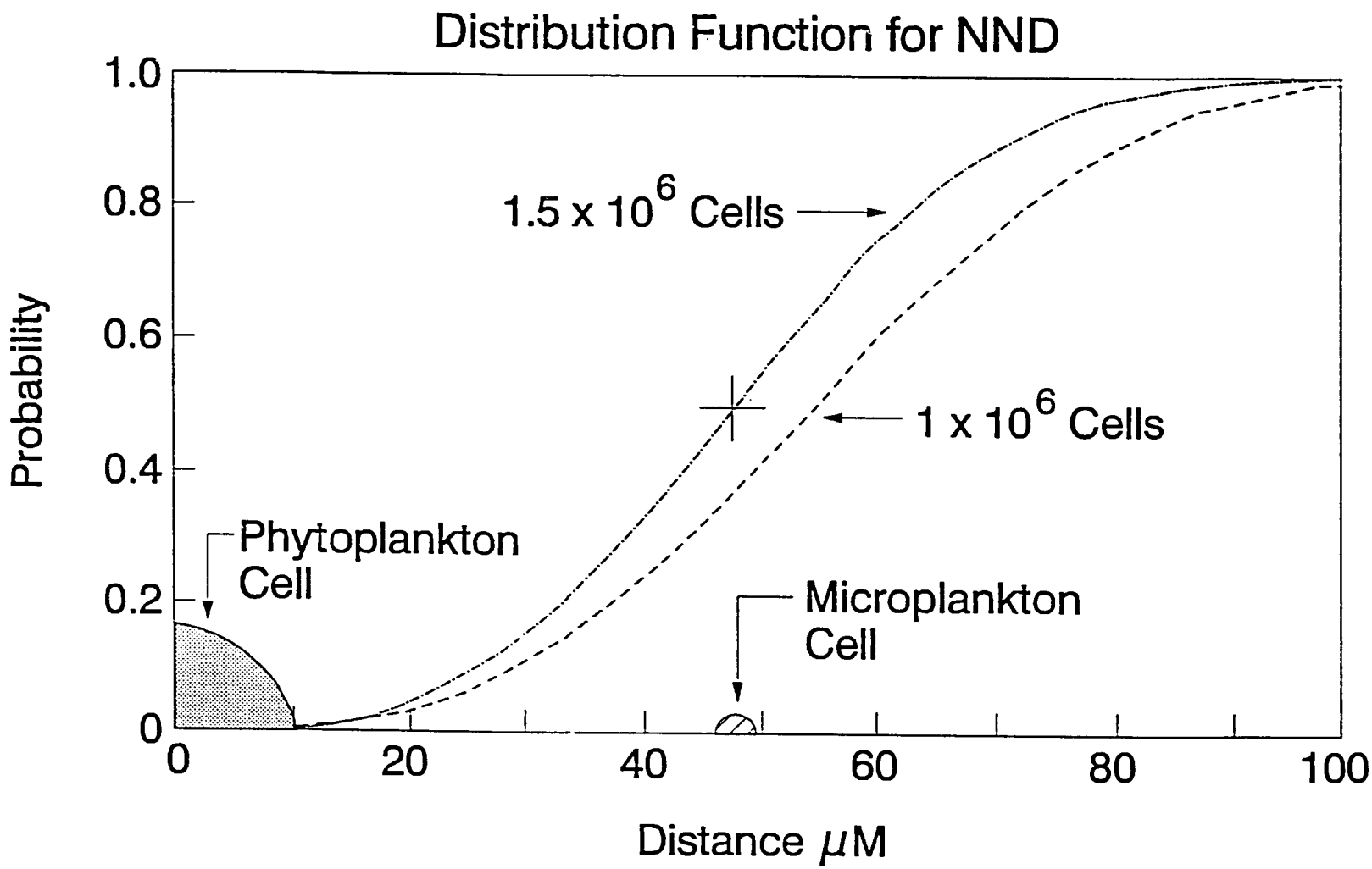


Figure 3. Probability distribution function for NND given a Poisson distribution and cell densities of $1 \times 10^6$ and $1.5 \times 10^6$ cells $cm^{-3}$. A phytoplankton cell and a microplanktonic heterotroph are superimposed at what might be a typical distance. The cross marks the mean NND for $1.5 \times 10^6$ random particle distance.

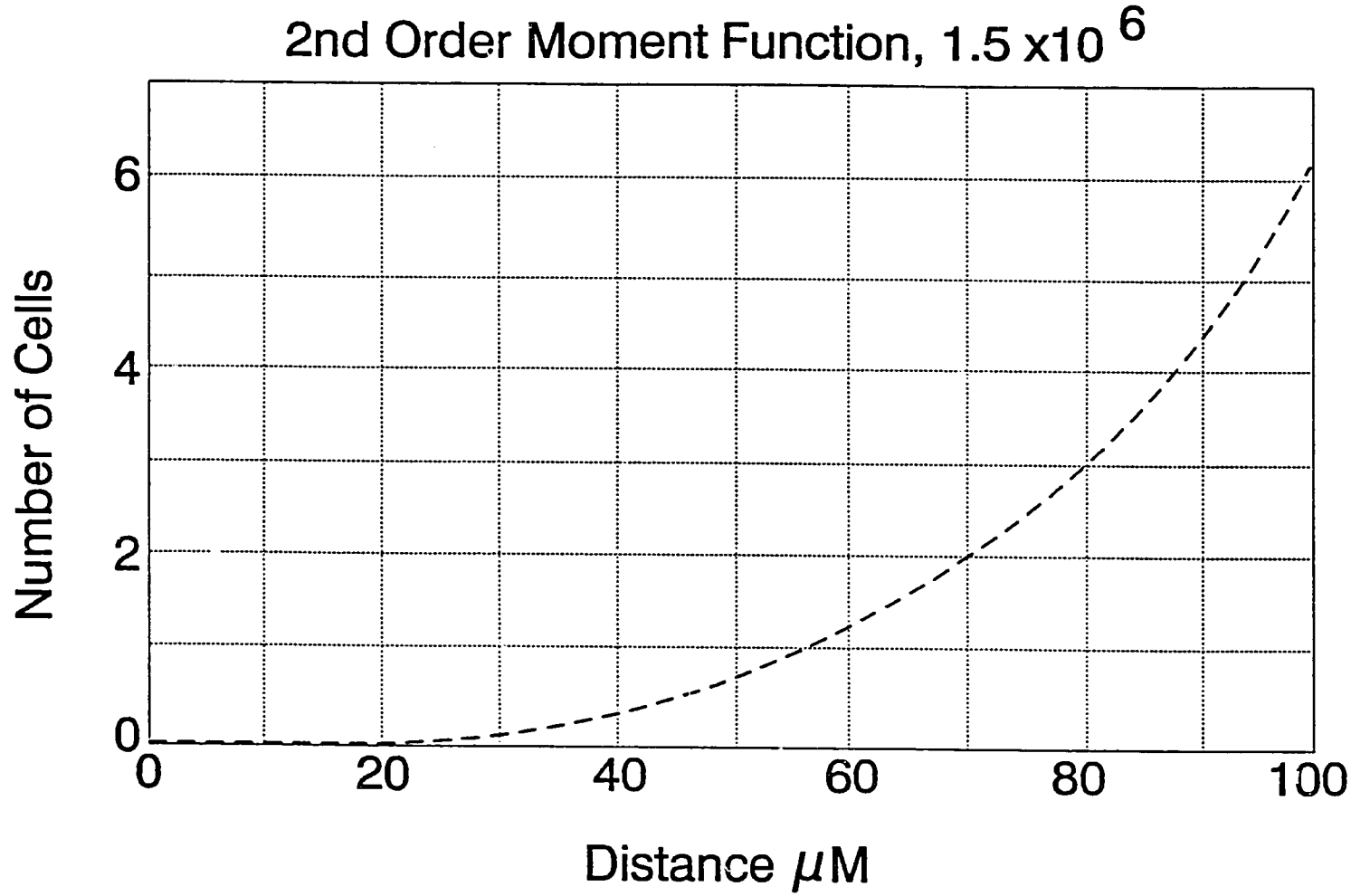


Figure 4. The product of the mean density and the RSOMF for a Poisson distribution with mean density $1.5 \times 10^6$ cells $cm^{-3}$. The RSOMF gives the mean number of cells within distance r from a particle. There are roughly six cells in a spherical shell between 50 and 100 microns.

the background concentration. Using this formula they compute that the algal-cell DOC microzone, 10 percent above background level would have a radius of ~1 mm.

As Mitchell et al. imply, the calculations of the magnitude of a microzone have not reached a level where they can be applied with certainty. In particular, there are many alternate assumptions regarding the factors that drive the temporal and spatial microzone volume. Among these are the temporal relation between the input and output of anabolites and catabolites respectively and the nature of the proportion between the volume of the microzone and the surface area per unit volume of the cell.

Uncertainty, regarding the microzone radius (both temporally and spatially) suggest treating the microzone radius as a variable and exploring how the volume fraction occupied by greater than background level metabolite might vary. The volume fraction occupied by the spheres of influence of the large autotrophs (based on a density of 400 individuals per $cm^{-3}$ is plotted in Figure 5). If we agree that a microzone radius of 100 $\mu m$ is "large", then we see that even at this large volume only .00250 of the volume is occupied by large autotroph microzones. On the other hand there are a very large number of small heterotrophs, so at a large microzone radius of 100 $\mu m$ and a concentration of microzone $1.5 \times 10^6$ heterotroph cells $cm^{-3}$, we would expect to find $(1.5 \times 10^6)$ $(2.5 \times 10^{-3})$ $= 3.75 \times 10^3$ small heterotrophs $cm^{-3}$ within autotroph microzones.

The volume fraction $p_h$ and the radius of the sphere of influence for a small heterotroph (having a density of $1.5 \times 10^6$ $cm^{-3}$) is plotted in Figure 6. By contrast the volume fraction increases

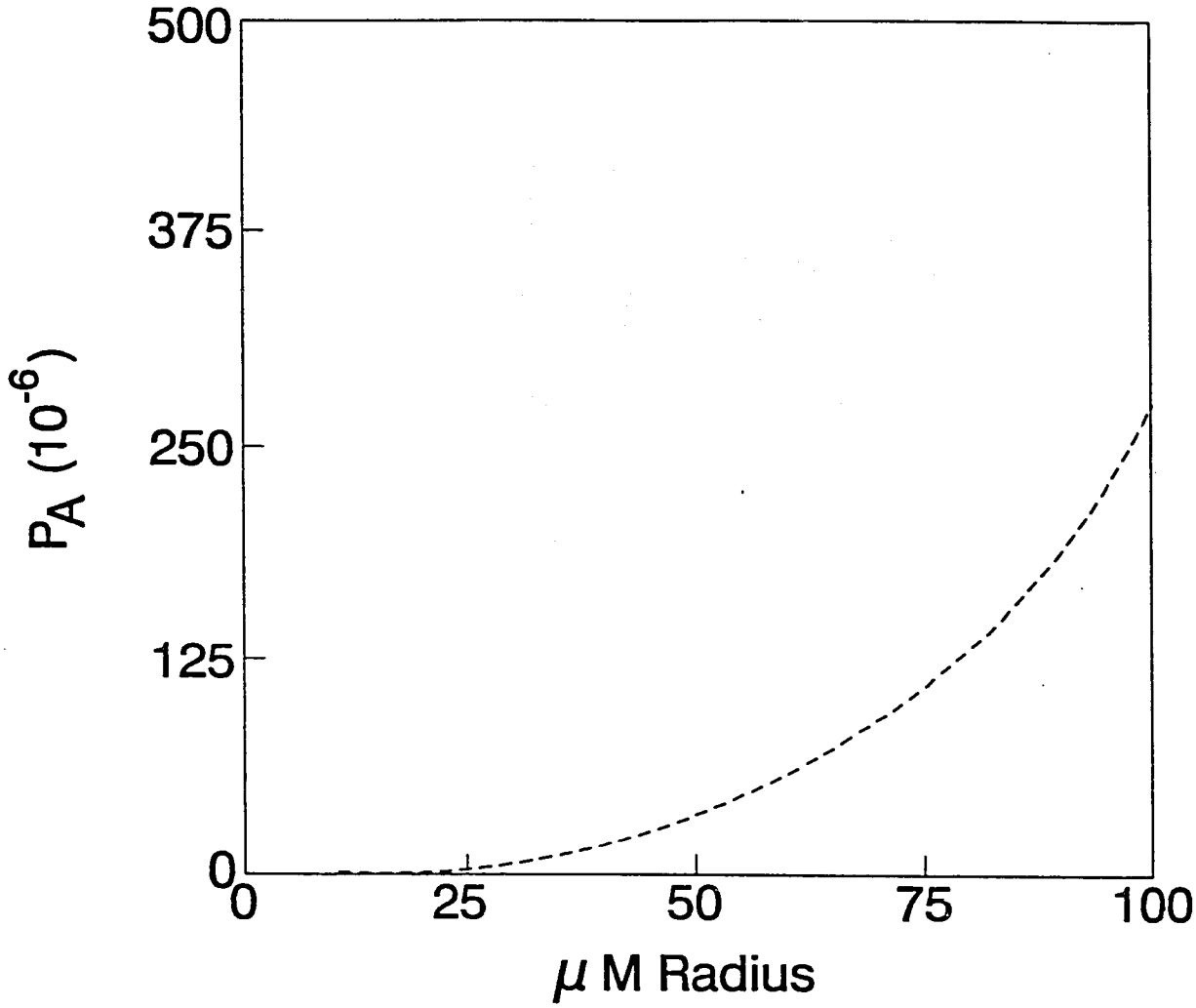


Figure 5. Relation between volume fraction, $P_A$, and radius of sphere of influence for autotroph where $\lambda_A$=400 $cm^{-3}$, and $\sigma_A^2 = \frac{1}{4}\mu^2$.

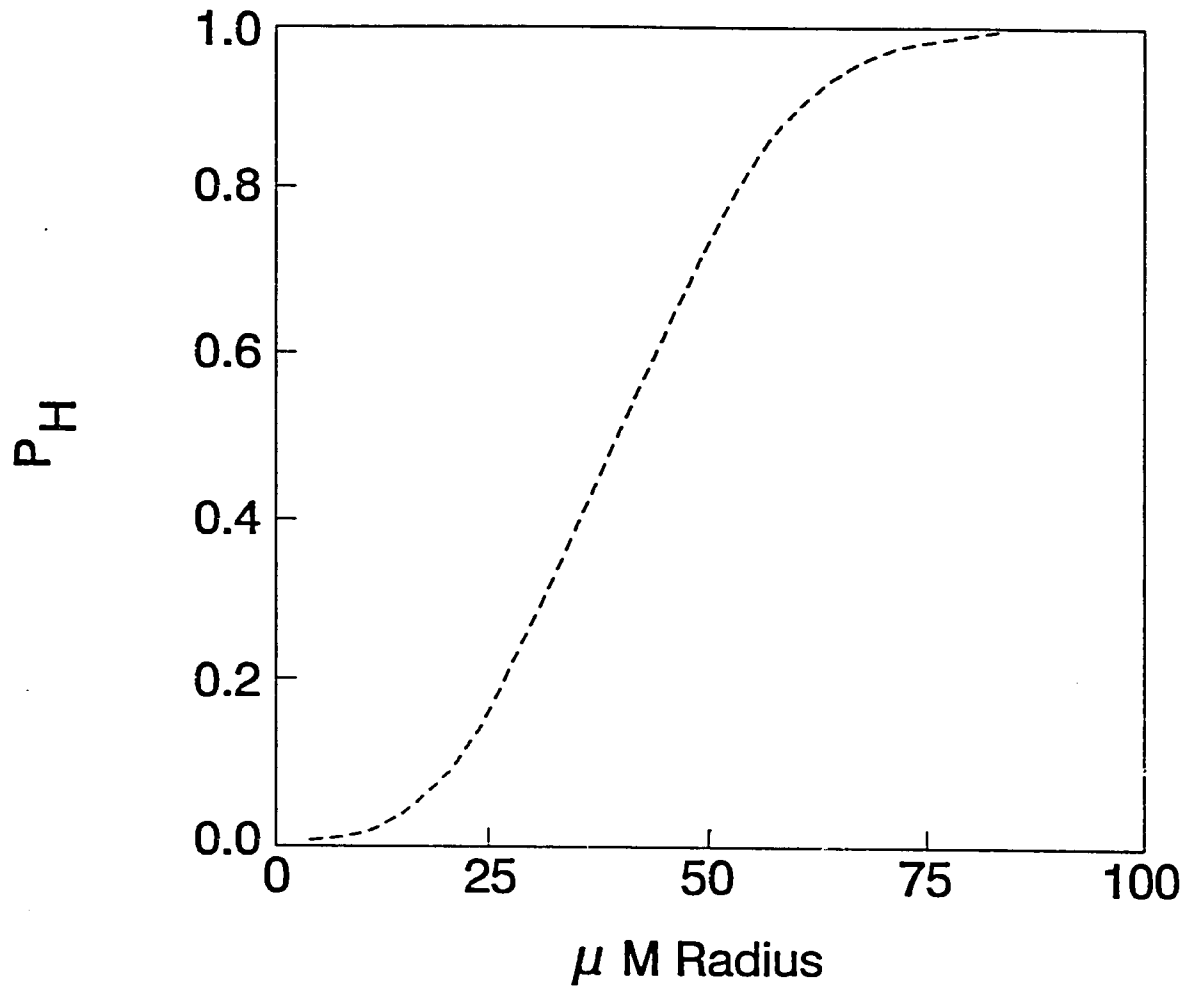


Figure 6. Relation between volume fraction $P_H$ and radius of sphere of influence for heterotroph, where $\lambda_H=1.5\times10^6$, and $\sigma_H^2=\frac{1}{4}\mu^2$.

much more rapidly by virtue of the fact that the numerical density of small heterotrophs is much greater than that of large autotrophs. Placing a large autotroph in a field of small heterotrophs leads to a sufficiently large expectation of intersections to expect interactions at higher than background levels.

The notion of the volume fraction can be used to estimate zones of synergy or "hot spots" between particles. To give an example of these calculations, we divide the pool of micro-plankton into two groups of $.75 \times 10^6$ cells $cm^{-3}$ each. The effect of the radius of the sphere of influence on the volume of intersection of spheres can be calculated using Eq (22). The results of the calculations are shown in Figure 7. The figure shows that the length of the radius has to be at least 20 $\mu m$ before interaction occurs. Between a radius of 20 $\mu m$ and a radius of 50 $\mu m$, roughly from 40 to 100 percent of the average NND, the volume occupied by catabolites from the two pools of cells taken jointly increases from 0 to 10 percent. The overlaps would increase if the radii were considered to have a variance. The crucial question regarding joint "hot spots" is whether conditions exist when microzones have radii greater than 20 $\mu m$. On the other hand such "hot spots" almost certainly exist given the arguments implied by Eq (6).

We conclude that in the, fixed point in time, random, particle-interaction "worst case" interparticle catabolites are donated and accepted at catabolite concentrations of greater than background levels. The over-all intensity and importance of the

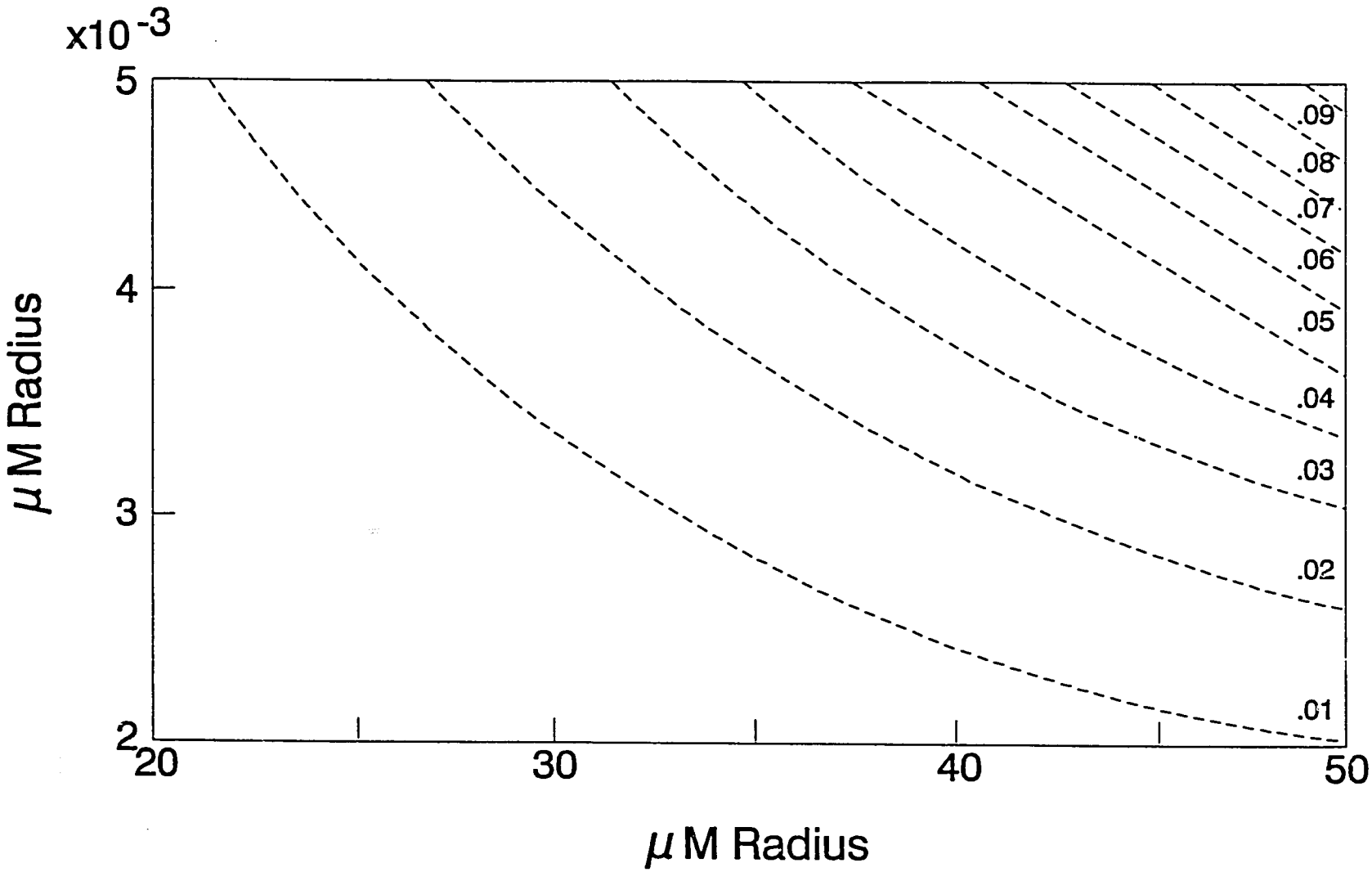


Figure 7. Volume fraction occupied by overlapping spheres of influence from two populations, each $.75 \times 10^6$ cells $cm^{-3}$ and with specified radius.

interaction depends upon the size of the microzones and the dynamics of geometry.

**Grazing--The Structure of Phytoplankton Patchiness.** Grazing (recent analyses include Costello et al, 1990 and Marrasé et al 1990) may be one of the more important classes of trophic transactions in the ecosystem, playing a key role in community metabolism, particularly in the transport of carbon to the lower ocean via fecal pellets. Surprisingly, data amenable to theoretical analysis of grazing are difficult to come by. This is because the most fundamental metric for studying such interactions involve the encounter of a grazer (e.g. a copepod) with an algal cell. Rather, than measuring encounters per-unit-time most studies have dealt with ingestion per unit time. Ingestion has been measured in a variety of ways that make comparisons difficult. These include measurements in terms of carbon, parts per million of particles, chlorophyll, in terms of behavioral responses, and numbers of prey per unit volume.

As pointed out by Rothschild (submitted) these approaches and the more classical approaches (e.g. Holling 1965) all are based upon a random distribution of prey relative to the predator even though there is ample evidence that distributions in the ocean are patchy. Accordingly, there is little data that can be used to study the spatial distribution of prey relative to the grazers. However, it is possible to infer the consequences of patchiness.

The idea is to take a copepod's world view of the distribution of its phytoplankton food. It is easy to show that a fixed or constant number of phytoplankton cells as might be represented by

actual counts, chlorophyll, behavioural response, etc. can be interpreted in a variety of ways by a copepod and that these ways depend as much upon the second-order properties of copepod distribution as the traditionally measured first-order properties.

First, we consider the copepods world view in a transition from random to patchy distribution for algal cells using a point-process theory. We suppose that the cells have intrapatch densities ranging from 0 to 700 cells $cm^{-3}$ and interpatch densities ranging from 0-700 cells $cm^{-3}$. For demonstration purposes we select the parameter, $\upsilon$=.75 (as $\upsilon$ decreases contours rotate to the vertical). The mean over-all densities and the NND's for these combinations are shown in Figure 8. Let us focus on a single mean density, 400 cells $cm^{-3}$, for example. At the point where the intrapatch and interpatch densities are equal to 400 cells, the distribution is random or Poisson, and the NND is roughly 750 $\mu$m. Transiting from a random to a patch distribution and constraining our observations to maintain a mean density of 400 cells $cm^{-3}$, we observe, for example, that at intrapatch densities of slightly more than 500 cells $cm^{-3}$ and interpatch densities of roughly 50 cells $cm^{-3}$ the NND drops to about 700 $\mu$m. The importance of this reduction in NND needs further study, however, from a copepod's point of view traveling at 720 cm hour means that it would increase its encounter rate on the average from about 9600 to 1029 cells per hour. Examining now the same 400-cell population isoline in connection with the RSOMF (Figure 9) shows that the RSOMF constant parameter increases from 400 to 500 as patchiness increases over the same range of intra/interpatch densities. The effect of increasing this

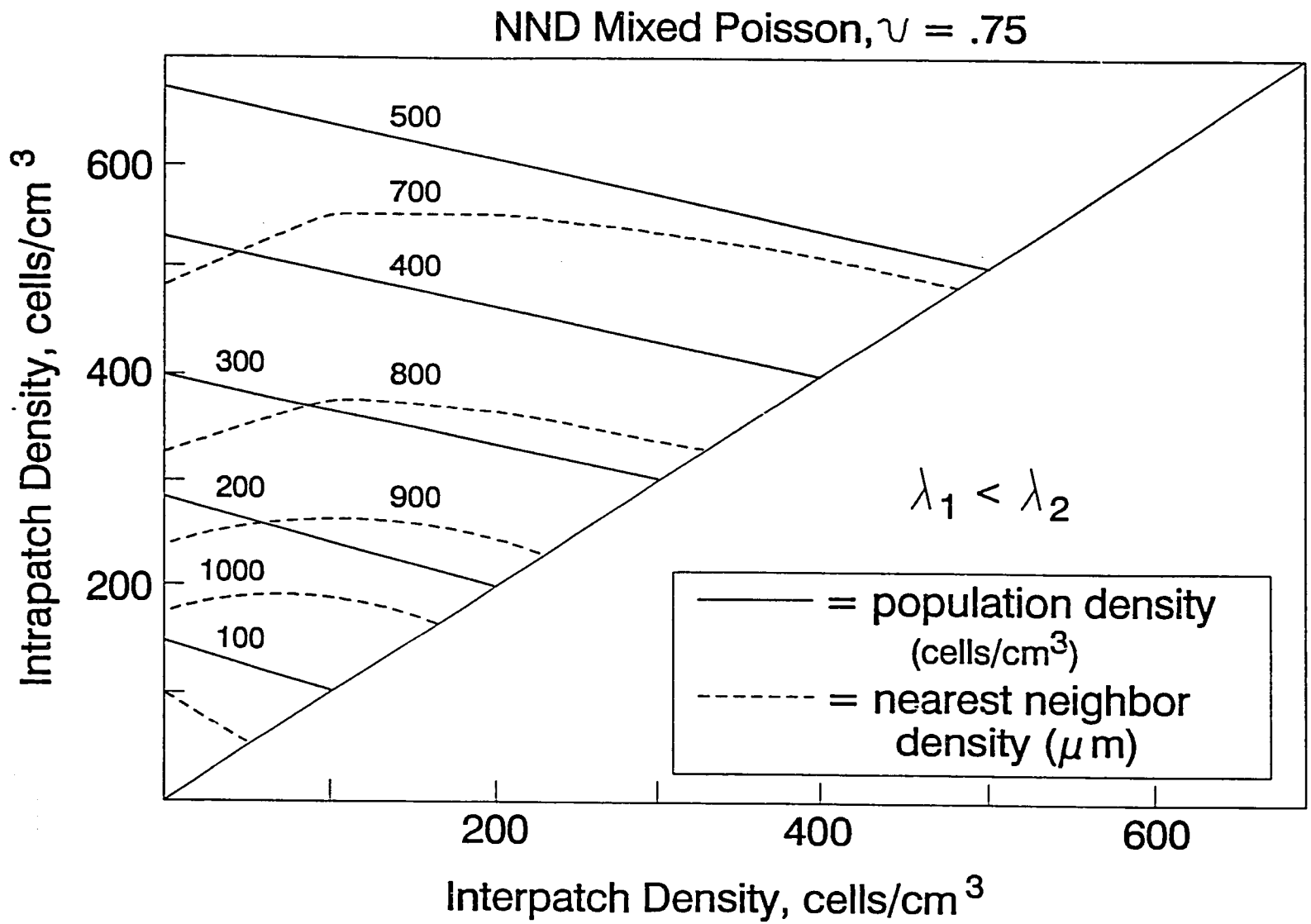


Figure 8. Contours of $\bar{\lambda}$ and NND for the mixed Poisson distribution with parameter ν=.75 for various intra and interpatch densities.

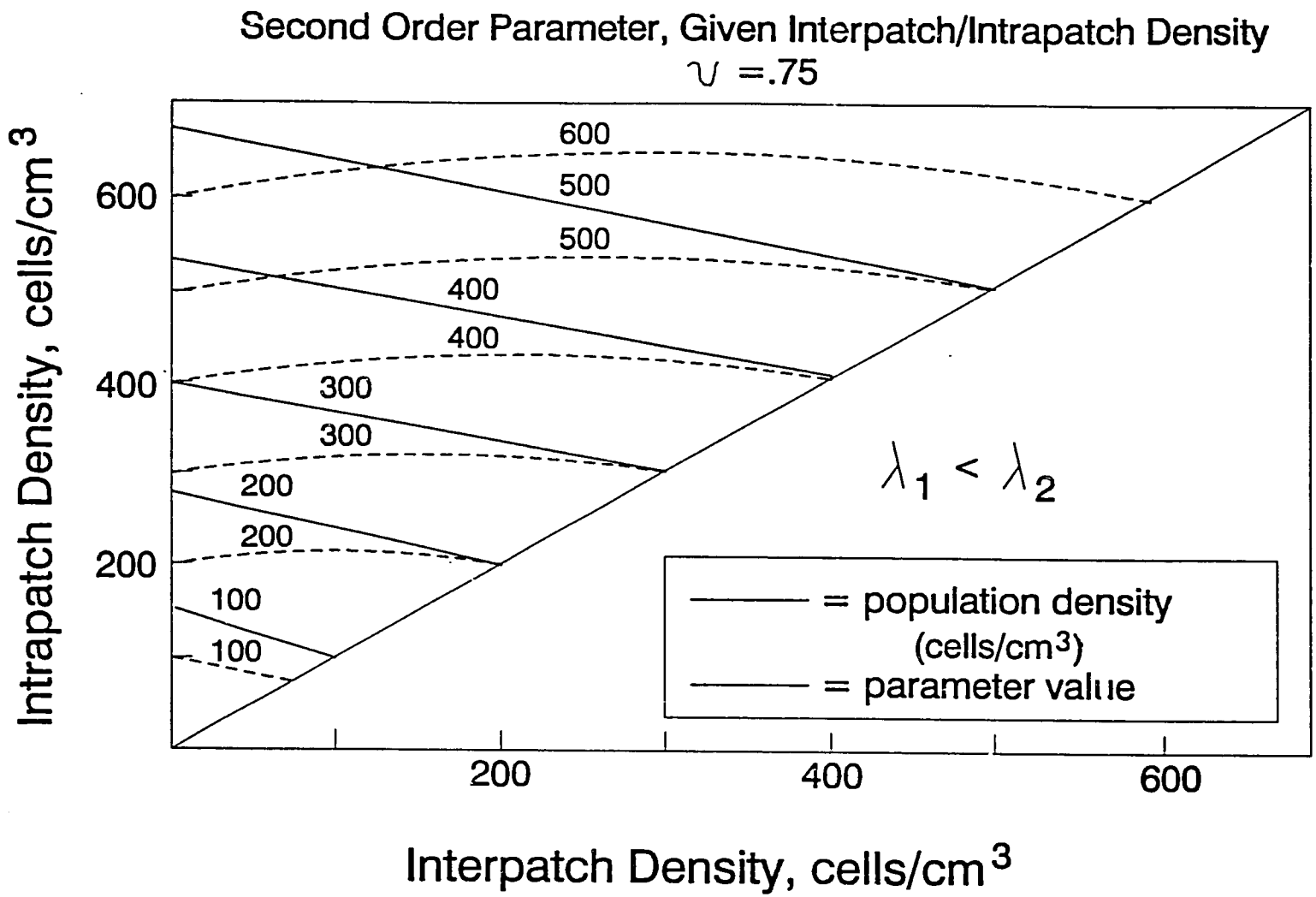


Figure 9. Contours of $\bar{\lambda}$ and the RSOMF with parameter ν=.75 for various intra and interpatch densities.

constant on the product of the density and the RSOMF is shown in Figure 10. It can be seen from the Figure that in a 720 cm search sphere the random and patchy distribution would yield population roughly $3x10^7$ and $4x10^7$ cells respectively. In other words, particle patch structure has increased the opportunity of contact in a fixed radius=720 cm search sphere by 33 percent. This brings to mind the question of random versus directed search on the part of the copepod in the sense that for the copepod to really take advantage of the increased numbers of cells in a patch environment it would have to find situations where the nearest neighbor distance was substantially less than say 700 $\mu$m. To put it more precisely, how does the copepod capitalize on MNND's in either a random or patchy distribution?

A different patch-structuring approach can be developed via RCS theory. In the point-process approach, a specified point process (e.g. a particular cluster process) with specified parameter values allocates particles to spatial points. Once the point process is chosen and once the parameters are set, the position of the points is determined automatically. In the RCS approach it is necessary to choose the germ distribution and its parameters and then the form of the grain, its distribution and parameter value(s). In other words, the RCS approach accommodates much more information than the point process approach, a blessing if the information is available, and a curse if it is not.

Accordingly, the allocation of points in RCS requires a greater range of decisions by the investigator. (We assume the

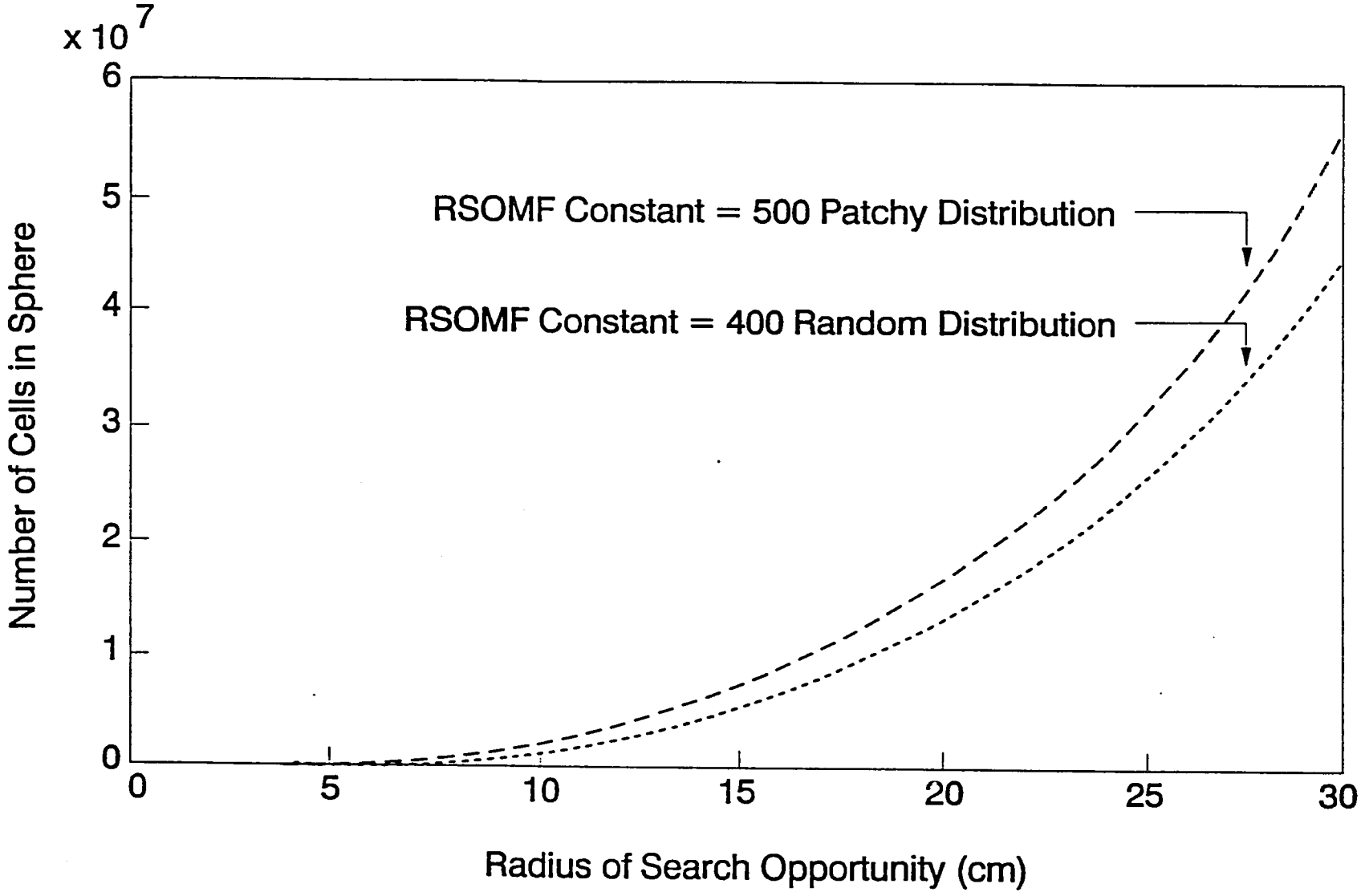


Figure 10. Product mean density and RSOMF showing the increase in feeding opportunities per unit radius of search sphere.

special case that each patch is spherical; the plankton particles are at fixed density inside a sphere, and nominally at zero density outside the sphere.) For example for any fixed volume such as $1M^3$ information needs to be supplied regarding,

1. The total number of cells
2. The number of patches
3. The volume fraction
4. The sphere radius and radius-variance
5. The allocation of cells to patches (e.g. fixed number or fixed density).

Determination of these properties is an important research undertaking which is necessary for an evaluation of the grazing problem.

To put the problem in more quantitative terms, consider Figure 11 which shows the volume fraction in the Boolean spherical model as a function of patch density, and patch radius. Because of the Boolean assumption patch density immediately gives the NND of patch centers whereas the patch volume is determined from its radius. Figure 11 shows how in an allocation scheme density of patch could be fixed; radius of patches could be fixed, and the volume fraction could be fixed. We can also see that when the volume fraction is low and the radius is low then there is an on the average separation of spheres, but when these variables are high the spheres coalesce.

Because the theory of RCS does not recognize the properties internal to the spheres the question of sphere coalescence is

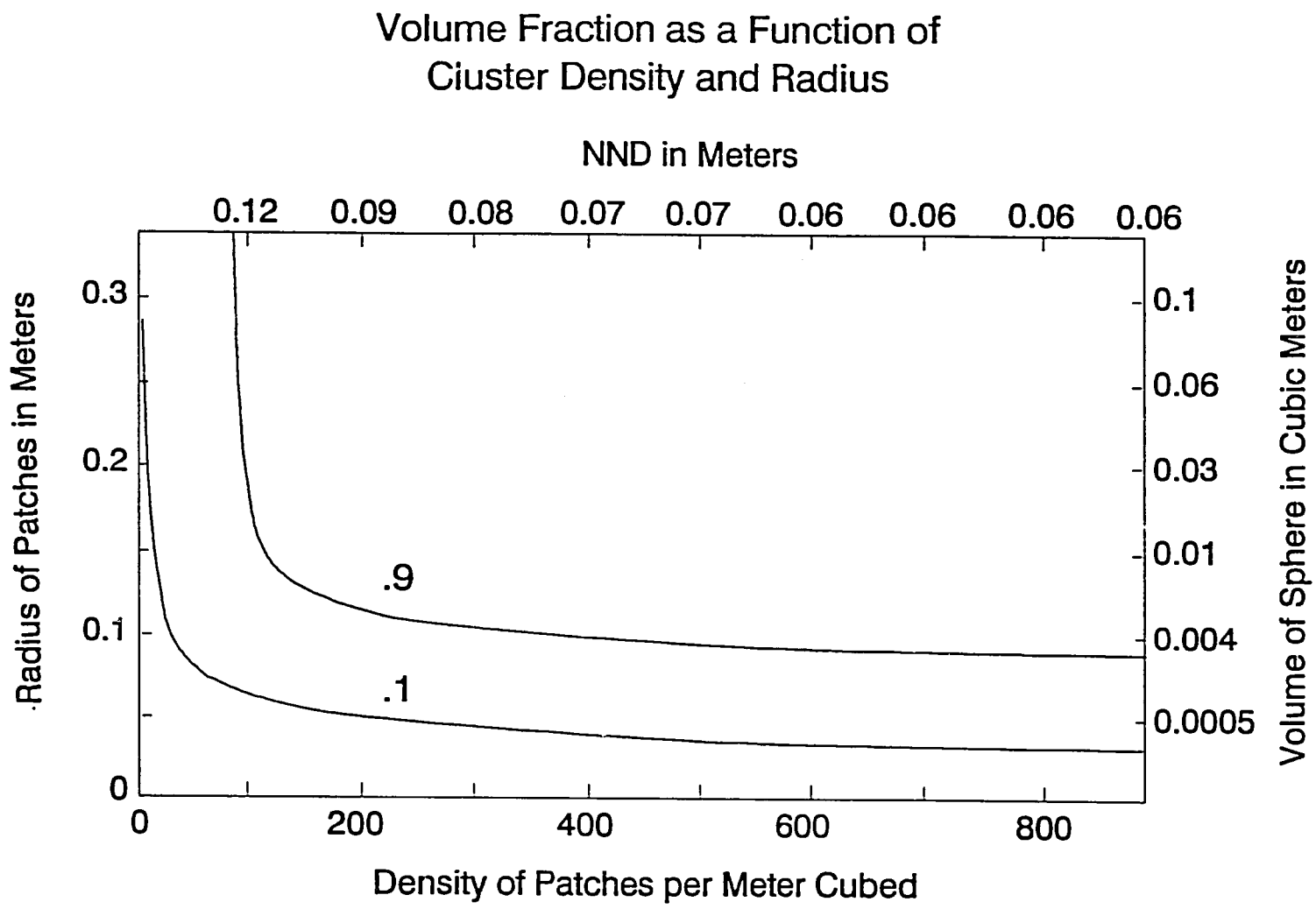


Figure 11. Boolean model, volume fraction as a function of patch radius or volume and patch density or interpatch center NND.

important. The requirements for coalescence can be seen in Figure 11. Minimum coalescence occurs at small values of volume fraction and small values of the patch radius to patch density ratio or to place the ratio in appropriate metric, $r^3/\lambda$.

The next problem is to allocate cells to spheres. An example of such an allocation using $200 \times 10^6$ cells $M^{-3}$ is shown in Figure 12. The hyperbolic relation is of course a constraint since given the density for the entire volume, all allocations must lie on the functional relationship. As an example $200 \times 10^6$ cells $M^{-3}$ (i.e. 200 cells $cm^{-3}$) are allocated to 50 and 500 patches $M^{-3}$ maintaining intra-patch densities of 400 and 800 cells $cm^{-3}$. For this particular example we divided the total number of cells $200 \times 10^6$ by either 50 or 500 giving the number of cells per patch--$4 \times 10^6$ or $.4 \times 10^6$ respectively. We then divided the number of cells per patch by the patch density (400 or 800 cells $cm^{-3}$) to obtain the patch volume. The patch radius was then determined directly from the volume. To obtain the covariance function it is necessary to assume some positive value for the radius variance, we let the standard derivation equal approximately one-half the mean radius. The results of the calculations are shown in Table 1.

We can see with this particular allocation scheme that if the within-patch density is fixed, then the within patch NND and the volume fraction is constant. On the other hand, if the number of patches per unit volume is fixed, then only the distance between the patches remains constant. Both the volume fraction and the integral scale vary over all four cases. Note, however, that

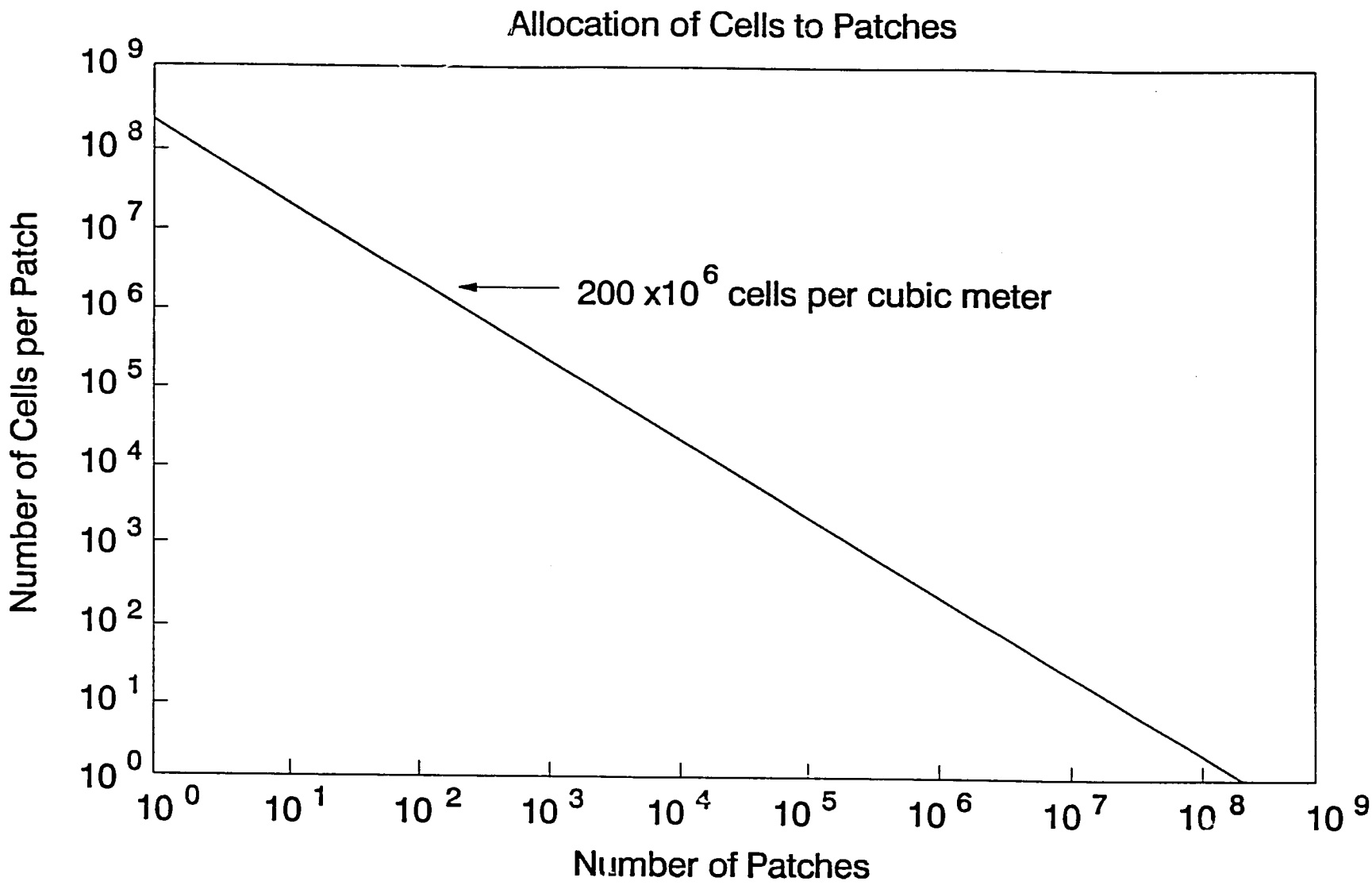


Figure 12. Allocation opportunities for allocating a fixed number of cells, $200 \times 10^6$ $M^{-3}$ to patches.

**Table 1.** Statistics representing an example of fixed allocations of $200 \times 10^6$ cells $m^{-3}$ and $50 \times 10^6$ cells $m^{-3}$ to 50 and 500 patches with 400 and 800 cells per patch. Note that if a grazer perceived only within patch density, then it could not distinguish among the four 400 cells $cm^{-3}$ $patch^{-1}$ or the four 800 cells $cm^{-3}$ $patch^{-1}$ allocations.

| Cells $m^{-3}$ | Cells $cm^{-3}$ $patch^{-1}$ | Patches $M^{-3}$ | Volume of Patch $CM^3$ | Patch Radius cm | Within Patch NND CM | Between Patch Center NND CM | Patch Std. Dev. cm. | Volume Fraction p | Integral Scale cm. |
|---|---|---|---|---|---|---|---|---|---|
| $200 \times 10^6$ | 400 | 50 | 10,000 | 13.365 | .0746 | 14.93 | 6.5 | .55 | 34 |
| | | 500 | 1,000 | 6.2035 | .0746 | 6.93 | 3.0 | .55 | 30 |
| | 800 | 50 | 5,000 | 10.608 | .0592 | 14.93 | 5.5 | .39 | 18 |
| | | 500 | 500 | 4.923 | .0592 | 6.93 | 2.5 | .37 | 15 |
| $50 \times 10^6$ | 400 | 50 | 2,500 | 8.410 | .0746 | 14.93 | 4.0 | | |
| | | 500 | 250 | 3.908 | .0746 | 6.93 | 2.0 | | |
| | 800 | 50 | 1,250 | 6.682 | .0592 | 14.93 | 3.0 | | |
| | | 500 | 125 | 3.102 | .0592 | 6.93 | 1.5 | | |

because in this example the ratio's $r^3/\lambda$ are large (in contrast with the heterotroph example) the propensity for overlap is also large (compare the patch NND with the patch radius). To take a different tack let us require a volume fraction smaller than p=.1 (cf Figure 11). We maintain 200 x $10^6$ cells $m^{-3}$ patch density at 50 patches $m^{-3}$. This means that we have all concentrations of $.8x10^{10}$ cells $m^{-3}$ or $.8x10^4$ cells $cm^{-3}$ within each patch a seemingly high concentration. In other words the problem is constrained: given what seem to be reasonable cell densities results in large spheres, large volume fractions, and a high degree of coalescence with a complex structure. On the other hand, if we fix the size of the patch at a small value relative to the density of patches, we have a small volume fraction, a low degree of coalescence, a simple structure, but a seemingly high concentration of cells. The grazer is faced with hypothetical search situation where the concentration of cells varies at relatively low levels between patch and patch intersection (at very high volume fractions multiple intersections are possible) at large volume fraction and situations where the concentration of cells varies to a much greater degree at small volume fractions.

The covariance function and the contact distribution contain information on overlap for the RCS. However, they do not contain information on heterogeneity within the sphere (should it exist, such as in the diffusion mediated heterotroph case) or interactions among the particles within the spheres. In a sense both the covariance function and the contact distribution can be thought of

in terms of particulate interaction whether or not spheres are completely isolated. The covariance function measures the distribution of distances <u>within</u> the volume fraction for all points inside all spheres. The contact distribution measures the intersphere distance in the sense that it involves the array of distances required to reach a sphere from a point external to a sphere. The covariance functions are plotted for each of the four cases in Figure 13. We can see that the property that the upper and lower ocean bounds of the covariance function are the volume fraction and the volume fraction squared. Inasmuch as the volume fractions depend only on the density of patches and their radius and variance and the volume of patches is held constant for 400 cells $cm^{-3}$ and 800 cell $cm^{-3}$ cases the upper and lower bounds for each of these cases is the same. However, in both instances the high number of smaller patches results in a much more rapid decline in the covariance function. Put another way, to use the jargon of Fourier analysis, the statistical power drops more rapidly as wave number increases with increased patch density.

The contact distribution for the four cases is shown in Figure 14. The contact distribution can be thought of in terms of the search opportunities of a grazing copepod. In this case the results are asymmetrical with those for the covariance function in the sense that there is more similarity within the number of patches per unit volume then between the number of patches per unit volume.

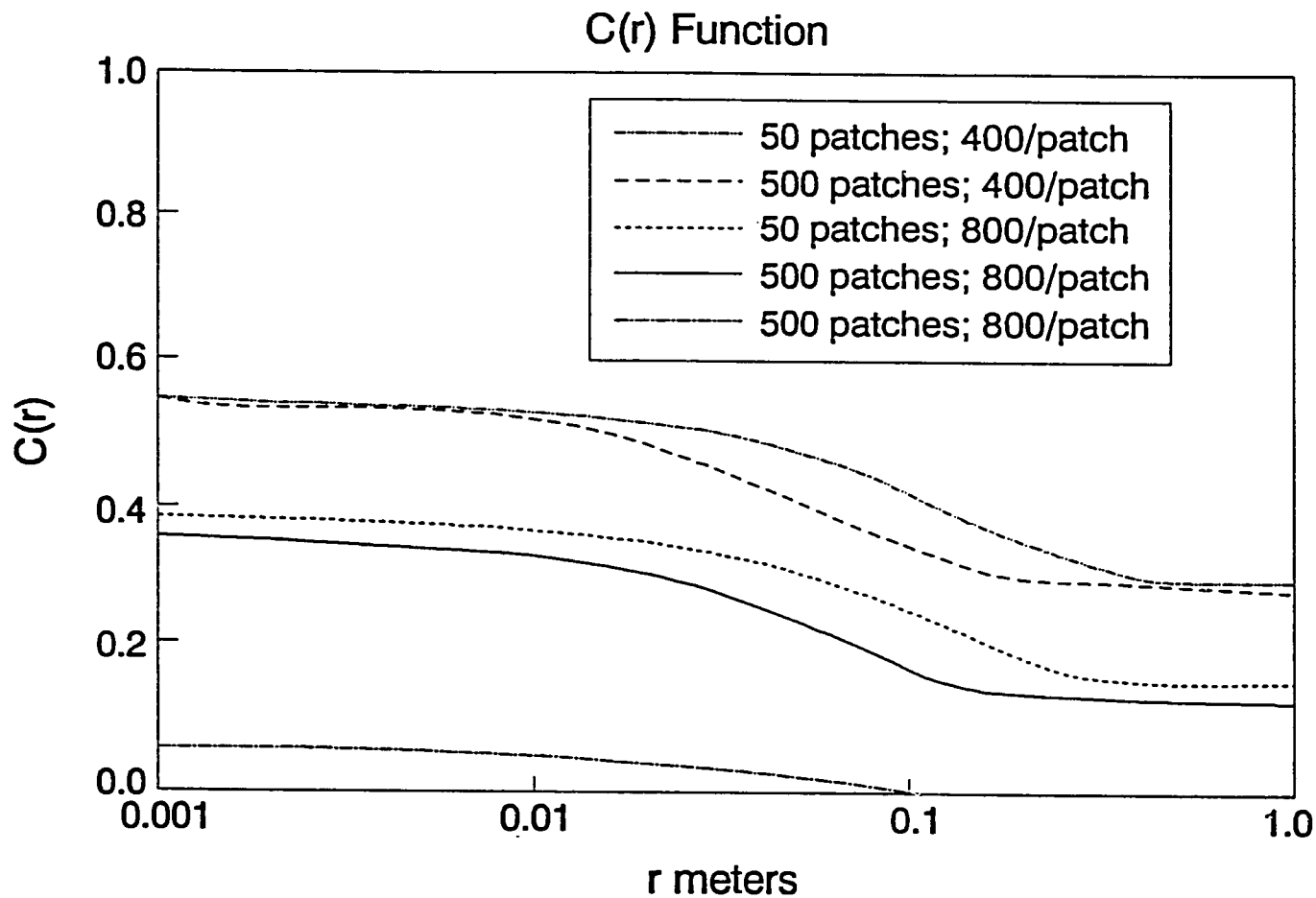


Figure 13. Covariance function as a function of distance from patch center for the cases indicated in Table 1. It is important to note that the Kolmogorov length scale can be superimposed on the x-axis. Its position would depend upon the magnitude of $\xi$.

Even though the overall density of phytoplankton cells is fixed, allocations to 500 rather than 50 patches $m^{-3}$ result in higher values of H(r) and hence lower values of $\bar{r}_h$. Given the particles allocation scheme high density patches are smaller and hence more distant.

In some ways more important than measuring the physical dimensions of particles spacing and its variability are the biological interpretations of such spacing. The covariance function and the contact distribution provide specifications that need to be taken into account when considering the search pattern of a copepod grazing on the phytoplankton cells. For example, if a copepod finds itself in the volume fraction occupied by a patch then the covariance function gives a statistical measure of the patch <u>centered on the copepod</u>. In a way the covariance specifies the turning radius that a copepod would want to maintain if it wanted to stay within a patch. The covariance function also gives a measure of "memory" in the sense that if the copepod moves farther than the integral scale, all traces of the patch are lost. In contrast, the contact distribution specifies the situation where the grazer is outside of a patch and is a measurement of the distance that would be necessary for the grazer to travel to find a patch.

The patch structure is critical to variability in the biological pump. On one hand, given a fixed number of cells per unit volume, patch structure regulates the variability in interencounter time of phytoplankton cells. If encounter times are

reduced more food is available per unit time. However, because of the functional response a reduced interencounter time may mean that less of the available food is eaten (Rothschild, submitted).

Two interesting applications arise, the first relates to chemosensation and the other relates to relative motion. First with respect to chemosensation or chemotactic search for food chemosensory distance thresholds can be superimposed on both the covariance and the contact distributions. As threshold differences change slightly small changes in probability occur. However, these could represent large changes in population properties because of expected value considerations. Second with respect to relative motion the kinetic forces on particles of water depend upon their distance apart and both the covariance and distance are statistically summarized by the covariance and contact distribution functions. The issues of chemotaxis and relative motion are discussed in subsequent sections.

<u>Micro-plankton and Grazer Search.</u> As shown in Figure 2, there is little chance for overlap in the NND of copepods and micro-plankton. On the other hand because the NND of the micro-plankton is of the order of 50 $\mu$m and the diameter of a copepod is orders of magnitude greater, it is difficult for a copepod to swim through the water without being in constant contact with micro-plankton. In fact a copepod proceeding at .2 cm $sec^{-1}$ through densities of $10^6$ micro-plankton $cm^{-3}$ will encounter $10^7$ micro-plankton $hour^{-1}$!

There are a number of studies that suggest that grazers find their food via chemotaxis. But if the DOC catabolized or leaked

from phytoplankton cells is rapidly diffused then chemical directional signals will certainly be obscured in the background-level chemical noise. On the other hand if the micro-plankton are metabolizing phytoplankton DOC then the chemical influence of the plankton patch would tend to extend farther than might otherwise be thought. In other words the micro-plankton serves as "repeaters" for phytoplankton catabolites and because of this, the grazer can steer more effectively to a patch of phytoplankton searching out particular MNND. The process would be even more efficient if the micro-plankton catabolism was actually triggered by either contact or catabolites from the grazer.

It is interesting to speculate on the structure of this system. In Figure 15 we portray the random distribution of 29 "signaling" micro-plankton points. We have connected this particular realization of points with a minimum-spanning tree (MST). The MST is computed such that the tree gives the path of the shortest distance among the points. For the copepod to use the MST to track the shortest distance the distance between the points has to be no greater than the signal detection capability of the copepod. If one such distance is too long then the switch is opened and the search has to be reinitiated. The affect of patch structure is to reorient the path. In Figure 16 we have moved some of the same points at random to the southwest corner of the plot. While some of the MST distances increase most decrease and the isotropic appearance of Figure 15 becomes anisotropic in Figure 16. It is likely that micro-plankton play an important role in the

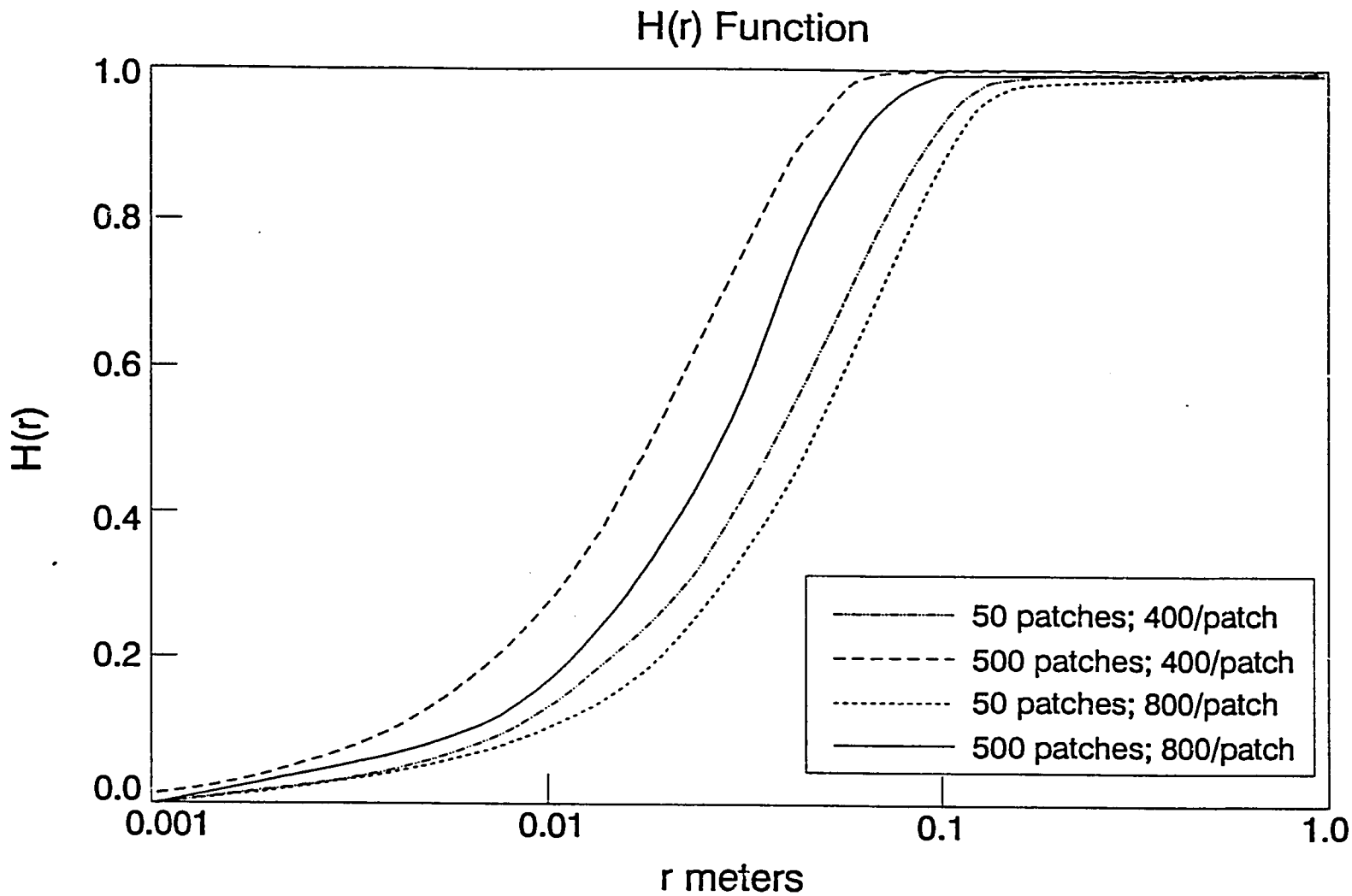


Figure 14. The "horizon" for a copepod not in a patch searching for a patch. H(r) is the probability of the nearest patch being at a distance r. Even though the overall density of phytoplankton cells is fixed, allocations to more patches result in higher values of H(r). Given the particular allocation algorithm higher density patches are smaller and hence more distant.

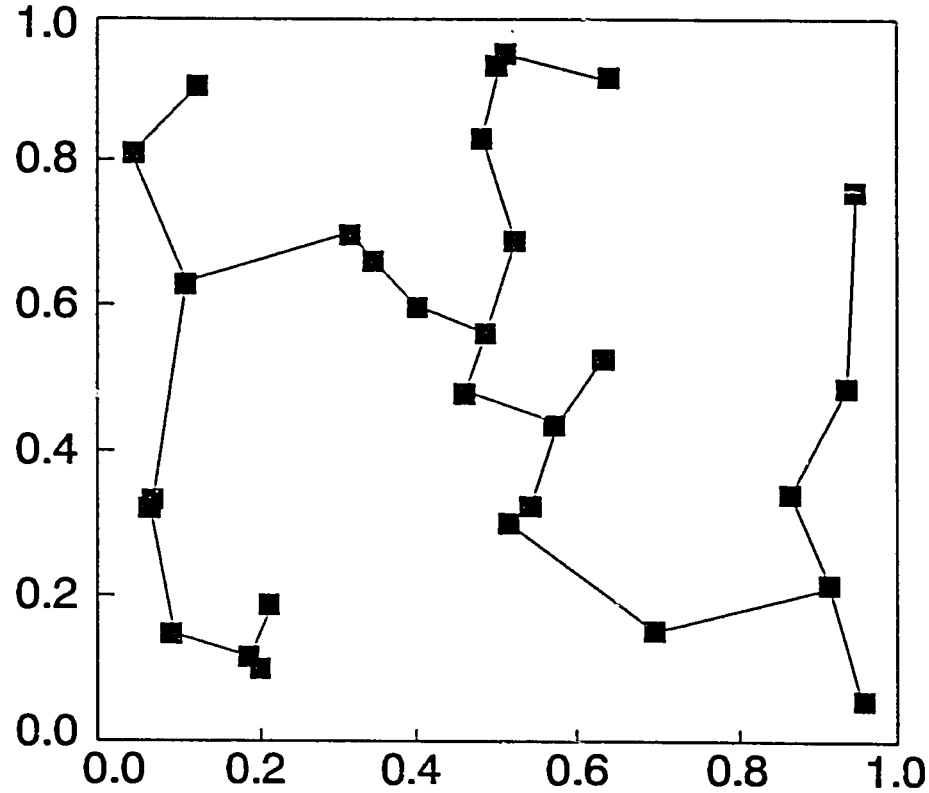


Figure 15. Minimum spanning tree connecting 29 randomly positioned microplankton points.

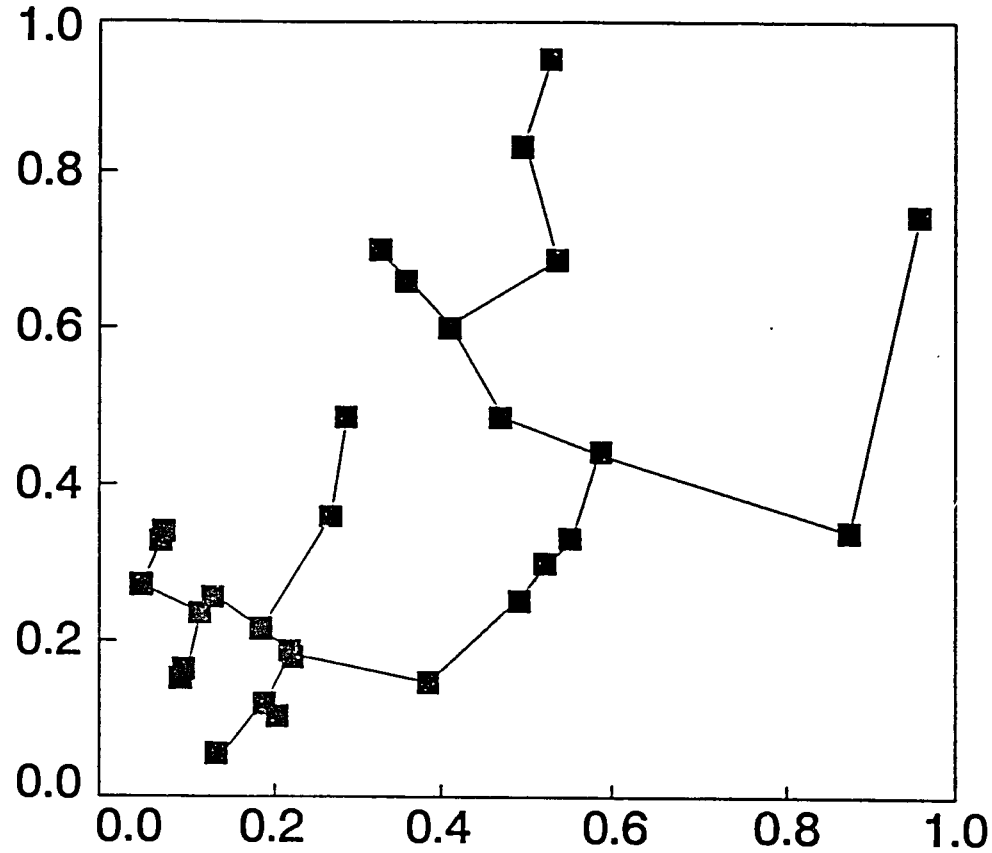


Figure 16. Minimum spanning tree connecting 29 points. Some of the points are the same as in Figure 15, but others were moved to the southwest corner using a chance process.

search for phytoplankton patches by grazers and that the patch structure of the micro-plankton may play an important role in these phenomenon.

## COUPLING WITH PHYSICAL PROCESSES

Physical processes are coupled with the integrative hierarchy in two fundamentally different ways. These are identified as Type I and Type II effects. Type I effects affect the physiology of the organism. Type II effects affect the interaction among organisms or their food resources. An example of a Type I effects are temperature. An example of Type II effect is the kinetic structure of the environment that would affect the relative velocity and hence the encounter rate of predator and prey. Another example of a Type II effect is the exposure of a phytoplankton cell to irradiance. We will concern ourselves with Type II effects since Type I effects are the subject of a considerable literature.

The fundamental question associated with Type II effects is how the particles sample the kinetic field. In a sense the particle distribution serves as an estimator of initial temporal values in a Lagrangian flow field. What are the statistical properties of the flow-field estimator? Estimator properties are generally related (among other things) to statistical accuracy (i.e. the interaction between bias and precision). These properties quantify the dynamics of interparticle distance and hence the propensity of particles to interact trophodynamically or behaviourly (as in the case of the grazer/large phytoplankton/ microplankton interactions.

An important point in this analysis is not whether the sampling process is biased or unbiased, but how the biodynamic structure evolves. The most primitive particles (in an evolutionary sense) move with the flow. In a random particle distribution they provide unbiased samples of flow. The most specialized organisms provide biased samples. In fact moving from primitive to specialized involves the evolutionary acquisition of motility. Because of this, from an individual-organism energetics perspective, it is necessary to take account of the net gains in fitness afforded by variability in the physical environment for immotile organisms and the net gains in fitness afforded by the interaction of motility and the physical environment. In other words, the position of particle results either from the kinetic field or from the kinetic field plus locomotion, two features which are critical to evaluating the effects of the physical environment on the organism.

To visualize the sampling notion consider N particles distributed in a plane vortex. Each particle samples a point in the vortex and each point is represented by a vector giving the direction and velocity at that point. We consider a patch as a more or less compact bounded collection of particles with an outer perimeter. All of the particles inside the perimeter are collectively called a patch. Some of the sampling possibilities are as follows (Figure 17):

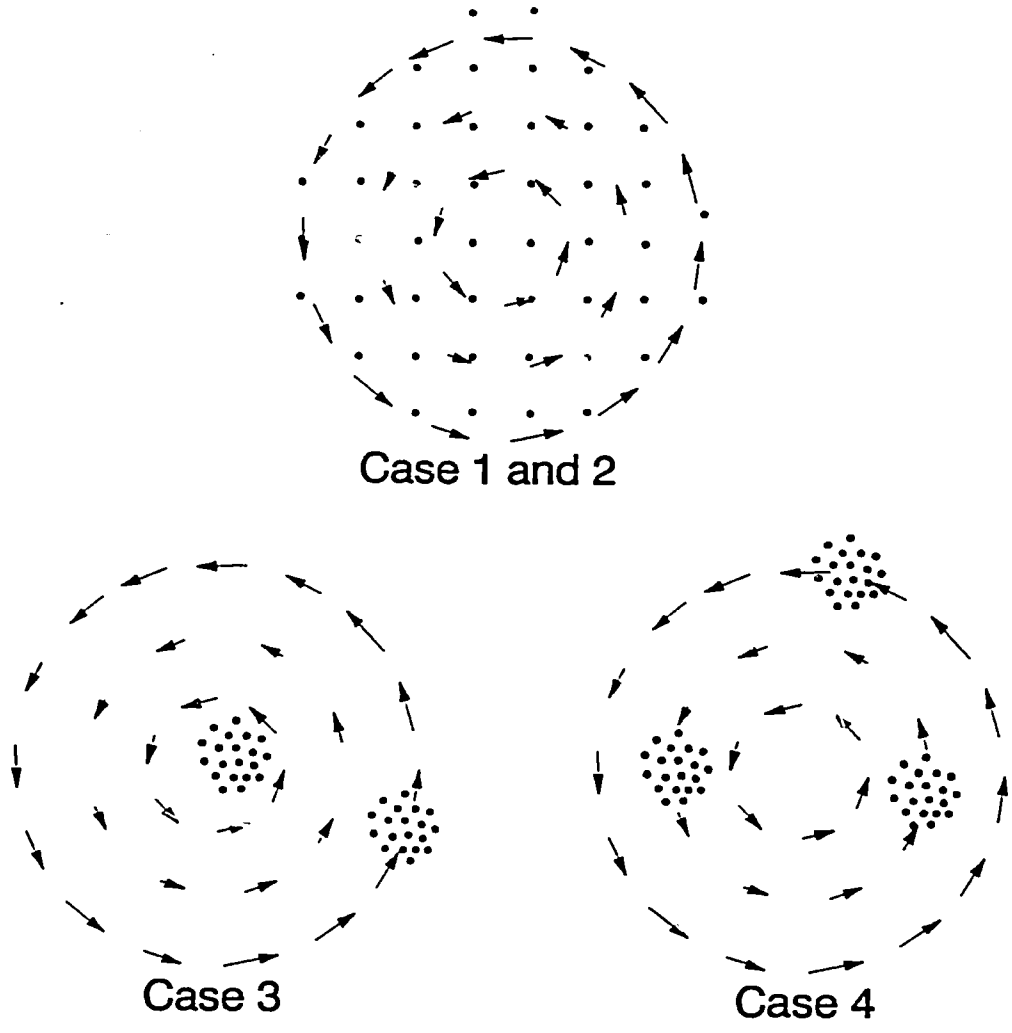


Figure 17. Influence of patch structure on flow sampling by particles. If the vortex is in the vertical plane then there are important implications with respect to sinking and exposure to irradiance.

1. The patch is roughly the same size as the vortex. The particles provide an unbiased estimate of vortex flow vectors.
2. The patch is larger than the vortex. The particles still provide an unbiased estimate of the flow vectors but with reduced precision.
3. The patch is much smaller than the vortex. Near the outside of the patch - the patch is advected east, west, south or north (or left, right, up and down). The patch can be deformed because of shear, although at the center of the vortex it simply rotates.
4. The behaviours of multiple patches in different configurations say with partitions 25, 25, 25, 25 or 50, 50 can be deduced from propositions 1, 2, or 3.

The main point is that stochastic geometry can be used to quantify the chance allocation of points to a flow field. As virtually all extant biological and theoretical studies implicitly imply that particles are randomly distributed, the use of stochastic geometry is a considerable advance, for as we have shown, a variety of first and second moment statistics (i.e. summarizations of chance data) provide compact summaries of the interparticle distances.

We are now prepared to give some precise interrelationships between the sampling process and the flow field. Any geometry $\Psi^*$ (say) samples the flow field such that at small scales, the velocity of each particle, or the force on a motile non-statistical

equilibrium particle is predictable. As Rothschild and Osborn have shown in fields of homogenous-and-isotropic turbulent flow the RMS uncorrelated velocities of two particles is a function of the turbulent kinetic energy dissipation rate, $\epsilon$, and the distance separating the particles.

But the distances separating particles for any $\Psi^*$ is naturally summarized by the covariance function Eq(19). Accordingly, we superimpose the Rothschild-Osborn function on the covariance function to demonstrate that the interaction among organisms are driven by patch scale given $\epsilon$ or that a change in $\epsilon$ can have a dramatic effect on patch interactions. Of course the problem is much more complex since $\epsilon$ is in itself a random variable -- possibly lognormal. In principle, then, it should, in addition to specifying the relative velocity of each particle be possible given any of the spatial distribution in this paper to derive the probability distribution of relative velocity as a function of two random variables problems.

The most interesting part of the analysis through is that we have sketched the linkage between basin-scale wind forcing (e.g. Dickson et al) and microscale patchiness. As Oakey and Elliot (1982), have pointed out (see also Sundby and Fossum 1990) $\epsilon$ is a function (of among other things) surface wind velocity.

There are of course other distance related effects. For example, changes in wind velocity affect many properties of the upper ocean in particular we assume that wind velocity affects the general magnitude of turbulent diffusion at the motion of organisms

relative to one another. The significance of diffusion relates to patch maintenance. We can infer that the conditions for patch maintenance are such that the length scale of a patch must be greater than a function of the diffusion coefficient, and the birth and death rate of the particles is the patch, viz.,

$$L > \phi\ (\alpha)$$
$$\alpha = \left(\frac{D}{\beta - \delta}\right) \tag{23}$$

where L is the patch dimension, D is the diffusion coefficient associated with the patch and $\beta$ and $\delta$ are birth and death rates respectively. This means that if birth and death rates do not change, but diffusion increases then the critical dimensions of the patch would need to increase. Similarly a decrease in the diffusion constant implies that smaller patches could be maintained. Further, as birth rates increased over death rates larger patches could be maintained.

## COUPLING THEORY AND OBSERVATION

An exemplification of plankton geometry finally makes it possible to couple in a logical way theory and observation. The basic idea is that validation of a theory on community-metabolism variability requires a capability to measure components of the system with well-defined and unambiguous methodology. The only way this can be done at the present time is via measurements of geometry, since it is difficult to put the measurements of rates in an unambiguous setting.

To firm up this idea consider a computer experiment on the metabolism of the upper ocean which proceeds for a large number of

time steps. A single time step is portrayed in Figures 18A, B. The initial geometry is $\Psi_0$. The geometry is shuffled by kinetic events driven by a hierarchy of basin and regional scale models (see G:50). The shuffling places predator and prey particles in new proximities to one another. In this intermediate geometry, $\Psi_{0+0.5}$, trophodynamics deletes prey particles and population dynamics modifies the mass of each remaining particle and its partitioning into somatic and reproductive biomass, creating the first step geometry.

Because there is considerable concern regarding how the "real world" should be measured the computer experiment also lends itself to facilitating the design of sensors and sampling-theoretical approach to making inferences about ecosystem structure. Simulated optic, acoustic, optic acoustic deployed in various ways (e.g. a moored optic/acoustic device or a satellite mounted radiometer) can be tested for optimality where the measure of performance compares $\Psi_i$ *with* $\psi_i$.. The computer experiment needs to be enhanced to take into account organisms motility and criteria for the choice of populations.

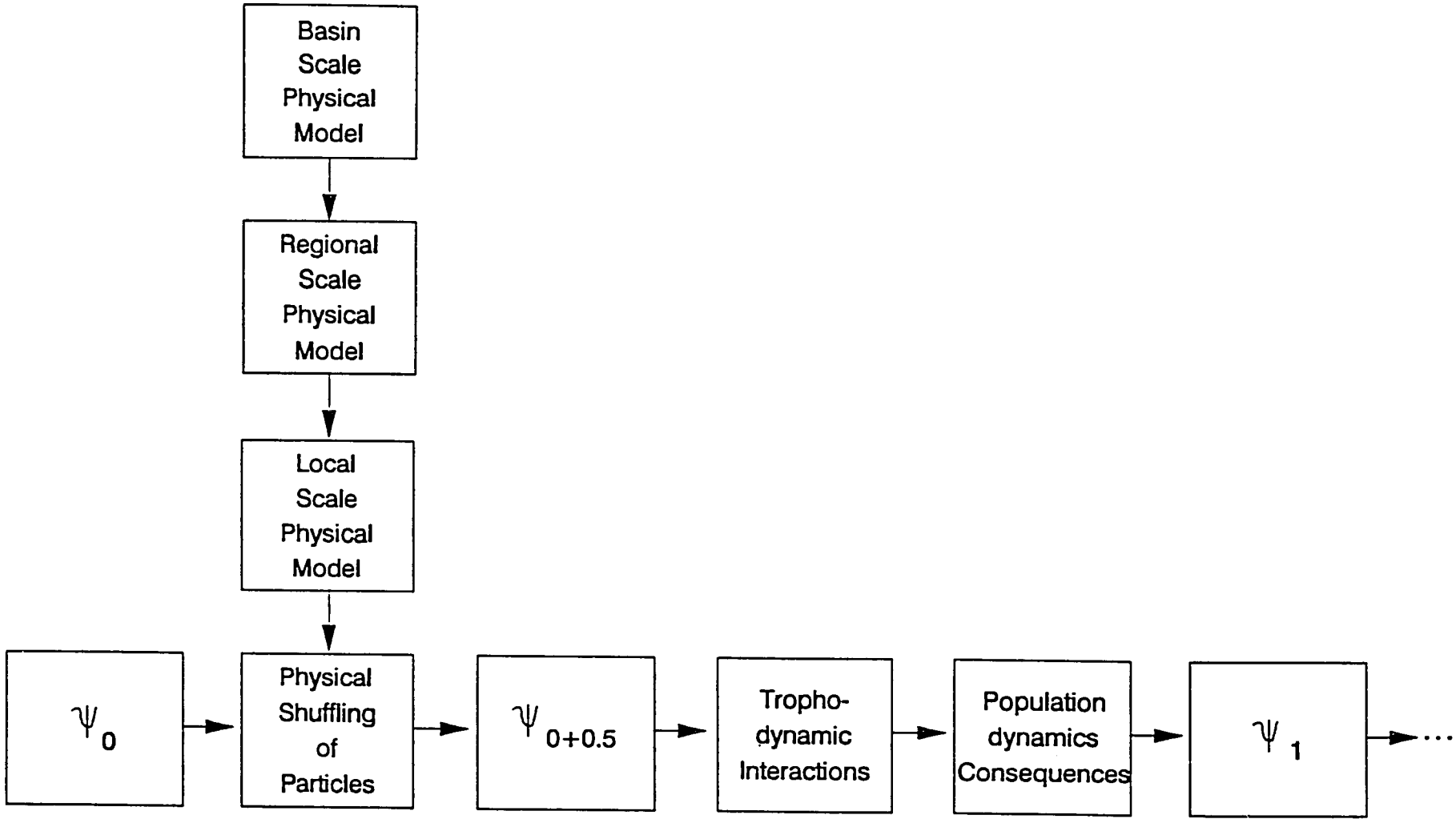


Figure 18a. One step flow in computer experiment linking physical models with geometry. The flow diagram shows how physics shuffling, trophodynamics, and population dynamics interact to form the dynamical events for geometrical change. Put another way these collective phenomena are the patch-genesis and patch-lysis mechanisms.

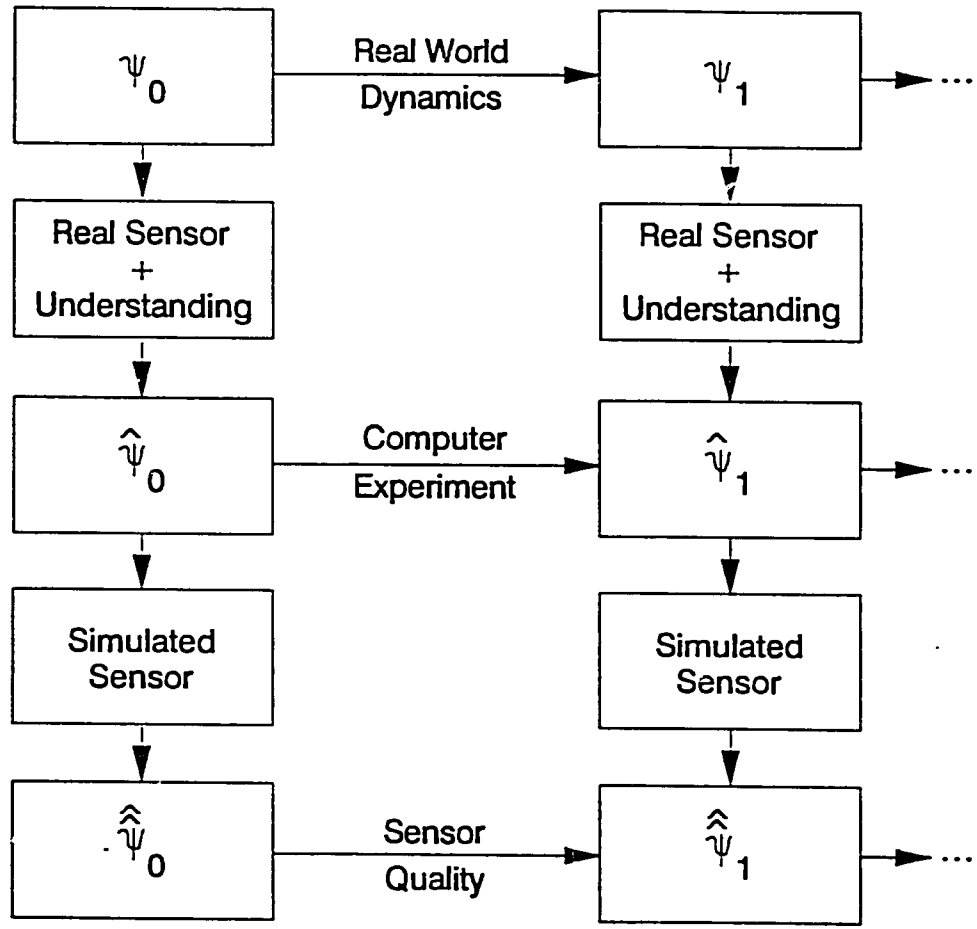


Figure 18b. Empirical theoretical coupling at time steps 0 and 1 assuming one-to-one temporal correspondence at all levels. This correspondence will generally need to be sacrificed.

## DISCUSSION

Upper-ocean community metabolism and its function as a biological-pump are critical elements in the attempt to explain the role of the sea in global-change phenomena. In addition to global change, other practical problems such as pollution and fishery management are of concern. With regard to pollution, forecasting the fates-and-effects of anthropogenic activity is a critical priority. These "fates and effects" must certainly depend upon variability in upper-ocean metabolism and the way that metabolism interacts with physical processes. Variations in community metabolism can be linked with variability in community-metabolism pathways (see e.g. LeFèvre and Frontier, 1988). As pathways change the relative importance of various sets of pollutants change. Knowledge of the changing pathways can have considerable impact on the public-policy decision process with respect to pollutants. With regard to fisheries, the saltatory occurrence of very large year classes and the consequent intervening small year classes set the stage for fishery management requirements. At present, capability to forecast the large year classes does not exist. If forecasts were available, fishery management could be much more efficient. The occurrence of the large year classes probably depends upon variability in metabolism.

The address of any these issues has always been difficult because observations generally seem to be associated with considerable variability. Does the unexplained variability arise from a truly entropic system, or on the other hand, does the

variability arise from sources of variability which are not taken into account. If such sources did exist, and they could be statistically controlled, then a materially improved understanding, and perhaps even predictability could be associated with the upper-ocean biodynamic process.

One critical source of variability that must play an important role in biodynamics and yet is scarcely understood is the coupling between biological and physical processes. We have shown that the existence of a non-random patch structure requires placing the plankton-particles in a physical framework. This framework begins with the geometrical distribution of the plankton. If the universality of feeding-scale patch structure can be demonstrated then it must be an important source of variability and a driving force in structuring the commonly observed larger-scale sampling or synoptic scale patchiness.

One of the interesting aspects of patch-structure study is the implication that the velocity (cf Goldman 1988) of the metabolic system in any fixed location, with any fixed set of organisms is controlled by interparticle distance. Proximity of microplankton (heterotrophs and autotrophs) and larger autotrophs increases primary production and increased primary production increases the particle available to grazers.

In studying the interactions among microplankton, we found that the understanding of temporal-spatial nature of microzones and the chemical kinetics with which they are formed was critical to determining the extent to which chemical communication among cells

occurred at greater than diffuse background levels. On one hand it appears that some cells are always close enough to exchange nutrients at greater than background levels. On the other hand, many of the cells are on the average, seemingly distant and so the frequency of functionally close proximity must depend upon the physical kinetics of the environment or particle motility. It is easy to conceive that any phenomena that promote either geometric or dynamic proximity create microbursts of productivity among the microplankton which are either spatially and temporally propagated or damped. The propagation of the microbursts results in the possible propagation of enhanced production in larger autotrophs, grazers, etc. In fact, such microburst propagation among the microplankton may even result in explaining the phenomenon of the periodic occurrence of very large year classes of fish.

In considering the world view of the zooplankton-grazer's food supply we found that even constraining the first-order abundance of phytoplankton cells to a constant value resulted in a rich variability of feeding conditions and even the genesis of "hot spots" of phytoplankton. The occurrence of a high-degree of patchiness suggests considerable variability in the nature of the <u>functional response</u> and in particular the efficiency with which a grazer ingests food, and symmetrically, the degree to which the phytoplankton cells are sequestered from predation. After all, the nature of <u>functional response</u>, <u>ceteris paribus</u>, controls the downwelling of organic carbon from the upper ocean.

In fact the opportunities for a grazer to find food seem to be

served least by a random search. But random search is in this case a anthropocentric frame of reference. To move out of that frame of reference it is necessary to understand, on one hand, the way in which phytoplankton cells are allocated to time-space points and, on the other hand, how the grazer moves from the anthropocentric world where $\bar{r}$ is a measure of proximity to another world where something like $\bar{r}^*$ is a measure of proximity. We have suggested that the microplankton might serve a function in moving from an $\bar{r}$ world to something like a $\bar{r}^*$ world.

Finally, we have shown that geometry provides an important coupling between trophodynamics and population dynamics and a setting in turbulent flow. Not taking account of geometry, could lead to important discrepancies in the encounter rate of predator and prey, for example. Perhaps more importantly we have shown that second-order spatial distribution couple directly with physical theory. In particular the RCS covariance function couples directly with the theory of homogeneous and isotropic turbulence.

The computer experiment is a plan of attack for the study of patch structure <u>dynamics</u> and emphasizes the <u>relative</u> simplicity of the study of patch-structure geometry. The geometry is fixed; particles are where they are; from a geometrical point of view there is no "why". However, without particle geometry as an initial and possible boundary condition, it is difficult to conceive a point of departure for setting the particles into motion, for considering the juxtaposition of predator and prey, or

for evaluating the resultant population-dynamic effects in terms of reproduction, growth and mortality. In fact the computer experiment is a point of departure for the study of what might be called "patchogenesis" and "patcholysis".

Stochastic geometry provides yet other opportunities. For example RCS theory provides other opportunity in the study of plankton dynamics. For example, volume scattering in acoustics and the clarity of water (the type I water clarity problem) are as dependent upon second order properties as might be articulated in RCS and point-process theory as the traditionally studied first-order properties. The theory of microzones which is perhaps one of the most critical and relatively least understood components of biodynamic theory is amenable to extensions of RCS theory, as well as immediate dynamic-like geometric consequences of geometry such as might be involved in the study of patch isolation.

The advancement of particulate theory requires study of two additional problems. These involve the motility and behaviour of organisms and the development of criteria to select populations for study. With regard to particle motility and behaviour, in general, all particles have an encounter-enhancing relative motion with respect to one another, simply by virtue of Stokes-law considerations. Many classes of particles are immotile and thus have no particular motility behaviour. On the other hand, even some of the smallest particles have propulsive mechanisms and behaviour with respect to food search (among other things). So a particle is at a space-time point either because it is carried to

that point in the process of interaction between its physical properties and the flow field, or because it has motility and behaviour that enable it to escape from statistical physical equilibrium. However, the escape from statistical equilibrium requires energy. At least some component of this energy affects the elaboration of reproductive biomass. Hence the energy required to escape from statistical physical equilibrium is of considerable population-dynamic significance particularly inasmuch as the energy expended by an organism to encounter prey is a function of the flow field enabling the causal linkage between flow and population dynamics.

With regard to the choice of populations, it is obvious that it is impossible to model all population in toto. This situation has given rise to the metabolic and other highly integrated approaches in the first place. The integrated approaches are justifiably criticized because they suppress population dynamics and the Type II physical effects as sources of variability. There is no easy answer to the choice of populations, but perhaps the problem can be reconfigured. One approach is to focus on the population dynamics process for a selected population. The process involves a number of populations it would be useful to study the extent to which the variability in any process was propagated or damped by associated populations. Another approach is the study of the variability structure of populations. For example an analysis of the eigenstructure of species composition or life tables reveals that there are generally biomass dominant and variability dominant

components in any mix of populations or age or stage classes. (Rothschild, in press). Rothschild and Ault (ms) found that in terms of both biomass and variability dominance the youngest age classes contained the bulk of variability. This suggests that a study of the eigenstructure of population variability might resolve focusing on first one subset of populations and then on another set of populations, possibly enabling insights into how the development of criteria of selecting manageable subsets of populations for study.

In conclusion the study of the particulate theory of the upper ocean and its coupling with physical processes is facilitated through the study of stochastic geometry. The geometrical representation is, however, just a first step needed to link the physical influence on particle distribution with tropho- and population-dynamics.

**ACKNOWLEDGEMENT**

Discussions with D. Capone were helpful in thinking about microplankton ecology. D.S. Robson read the paper and provided helpful insights. Huaxing Li computed the covariance and contact distribution functions.

## APPENDIX I

Integration of Eq(4) and Eq(9) involves integration of a gamma function. Solutions are not available in simple tables. The appropriate formula is,

$$\int_0^\infty x^m e^{-ax^n} dx = \frac{1}{na^{(m+1)/n}} \Gamma\left(\frac{m+1}{n}\right)$$

## LITERATURE CITED


Allee,W.C., Emerson,A.E., Park,O., Park,T., and Schmidt,K.P. (1949) Principles of Animal Ecology. W.B. Saunders Company, Philadelphia; 837pp.

Costello,J.H., Strickler,J.R., Marrasé,C., Trager,G., Zeller,R., and Freise,A.J. (1990) Grazing in a trubulent environment: Behavioral response of a calanoid copepod, *Centropages hamatus*. Proc. Natl. Acad. Sci. USA, Vol. 87, pp. 1648-1652.

Dickson,R.R., Kelly,P.M., Colebrook,J.M., Wooster,W.S., and Cushing,D.H. (1988) North Winds and Production in the Eastern North Atlantic. J.Plank.Res., 10, 151-169.

Fasham,M.J.R. (1978a) The Statistical and Mathematical Analysis of Plankton Patchiness. Oceanogr.Mar.Biol.Ann.Rev., Vol. 16, pp. 43-79.

Fasham,M.J.R. (1978b) The Application of Some Stochastic Processes to the Study of Plankton Patchiness **In** Spatial Pattern in Plankton Communities edited by J.H. Steel. NATO Conference Series IV: Marine Sciences. Plenum Press, New York, pp. 131-156.

Gerritsen,J. and Strickler,J.R. (1977) Encounter probabilities and community structure in zooplankton: A mathematical model. J.Fish.Res.Board Can., Vol. 34, pp. 73-82.

Goldman,J.C. (1988) Spatial and Temporal Discontinuities of Biological Processes in Pelagic Surface Waters, **In**, Toward a Theory on Biological-Physcial Interactions in the World Ocean, Edited by B.J. Rothschild. NATO ASI Series C:Vol. 239, pp.273-296. Kluwer Academic Publishers, Boston.

Holling,C.S. (1965) The functional response of invertebrate predators to prey density and its role in mimicry and population regulation. Mem.Entomol.Soc.Canada, 45:1-60.

Jackson,G.A. (1987) Physical and Chemical Properties of Aquatic Environments, **In**, Ecology of Microbial Communities, Edited by M. Fletcher, T.R.G. Gray and J.G. Jones. pp.213-233. Cambridge University Press.

Jahnke,R.A. (1990) Ocean Flux Studies: A Status Report. Review of Geophysics, Vol.28, No.4. pp.381-398. American Geophysical Union.

LeFèvre,J. and Frontier,S. (1988) Influence of temporal characteristics of physical phenomena on plankton dynamics as shown by North-West European marine ecosystems, **In**, Toward a Theory on Biological-Physical Interactions in the World Ocean, Edited by B.J.Rothschild. NATO ASI Series C:Vol. 239, pp.245-272. Kluwer Academic Publishers, Boston.

Longhurst,A.R. and Harrison,W.G., (1989) The biological pump: Profiles of plankton production and consumption in the upper ocean. Prog.Oceanogr., 22, 47-122.

Marrasé,C., Costello,J.H., Granata,T., and Strickler,J.R. (1990) Grazing in a trubulent environment: Energy dissipation, encounter rates, and efficacy of feeding currents in *Centropages hamatus*. Proc.Natl.Acad.Sci. USA, Vol.87, pp. 1653-1657.

Mitchell,J.G., Okubo,A., and Fuhrman,J.A. (1985) Microzones surrounding phytoplankton form the basis for a stratified marine microbial ecosystem. Nature, Vol.316, pp. 58-59.

Oackey,N., and Elliot,J. (1982) Dissipation within the surface mixed layer. J.Phys.Ocean., Vol.12, pp. 171-185.

Pielou,E.C. (1977) Mathematical ecology. New York: Wiley.

Rothschild,B.J. (1990 submitted) The Role of Food Signals in the Regulation of Marine Populations.

Rothschild,B.J. (1986) Dynamics of Marine Fish Populations, Chapter 8: The Population-Dynamics Process. pp. 218-236. Harvard University Press.

Rothschild,B.J., and Ault,J.S. ms. (1990) The Eigenstructure of Life Tables.

Rothschild,B.J., and Osborn,T.R. (1988) Small-scale turbulence and plankton contact rates. J.Plank.Res., Vol.10, No.3 pp. 465-474.

Stoyan,D., Kendall,W.S. and Mecke,J. (1987) Stochastic Geometry and Its Applications. John Wiley and Sons, New York. 345p.

Sundby,S., and Fossum,P. (1990) Feeding conditions of Arcto-norwegian cod larvae compared with the Rothschild-Osborn theory on small-scale turbulence and plankton contact rates. J.Plank.Res.,Vol.12, No.6,pp.1153-1162.

Walsh,J.J. (1981) Shelf-Sea Ecosystems, In Analysis of Marine Ecosystems Ed. A.R. Longhurst. Academic Press Inc., London. pp.159-196.